ความไม่ต่อเนื่องของค่าความร้อนจำเพาะอิเล็กทรอนิกส์ของตัวนำยวดยิ่งอุณหภูมิสูงที่อุณหภูมิวิกฤต

นายสุชาติ เกศกมลาสน์

หอสมุดกลาง สถาบันวิทยบริการ จุฬาลงกรณ์มหาวิทยาลัย

วิทยานิพนธ์นี้เป็นส่วนหนึ่งของการศึกษาตามหลักสูตรปริญญาวิทยาศาสตรมหาบัณฑิต

สาขาวิชาฟิสิกส์ ภาควิชาฟิสิกส์

คณะวิทยาศาสตร์ จุฬาลงกรณ์มหาวิทยาลัย

ปีการศึกษา 2542

ISBN 974-333-903-5

ลิขสิทธิ์ของจุฬาลงกรณ์มหาวิทยาลัย

I 19011878

ELECTRONIC SPECIFIC HEAT DISCONTINUITY AT CRITICAL TEMPERATURE OF HIGH-T_c SUPERCONDUCTORS

Mr. Suchat Kaskamalas

A Thesis Submitted in Partial Fulfillment of the Requirements for the Degree of Master of Science in Physics

Department of Physics

Faculty of Science

Chulalongkorn University

Academic Year 1999

ISBN 974-333-903-5

Thesis Title	Electronic Specific Heat Discontinuity at Critical Temperature of High-T_c Superconductors
By	Mr. Suchat Kaskamalas
Thesis Advisor	Professor Virulh Sa-yakanit
Thesis Co-Advisor	Professor Suthat Yoksan

Accepted by the Faculty of Science, Chulalongkorn University in Partial Fulfillment of the Requirements for the Master's Degree.

.....Dean of Faculty of Science
(Associate Professor Wanchai Phothiphichitr, Ph.D.)

THESIS COMMITEE

.....Chairman
(Associate Professor Kitt Visoottiviseth, Ph.D.)

.....Thesis Advisor
(Professor Virulh Sa-yakanit, F.D.)

.....Thesis Co-Adisor
(Professor Suthat Yoksan, Ph.D.)

.....Member
(Pornthep Nisamaneephong, Ph.D.)

.....Member
(Associate Professor Wichit Sritrakool, Ph.D.)

สุชาติ เกศกมลาสน์ : ความไม่ต่อเนื่องของค่าความร้อนจำเพาะอิเล็กทรอนิกส์ของตัวนำยวดยิ่งอุณหภูมิสูงที่อุณหภูมิวิกฤต. (ELECTRONIC SPECIFIC HEAT DISCONTINUITY AT CRITICAL TEMPERATURE OF HIGH-T_C SUPERCONDUCTORS) อ. ที่ปรึกษา : ศ. ดร. วิรุฬห์ สายคณิต, อ. ที่ปรึกษาร่วม : ศ. ดร. สุทัศน์ ยกส้าน , 70 หน้า. ISBN 974-333-903-5.

จุดมุ่งหมายของวิทยานิพนธ์นี้คือเพื่อศึกษาความไม่ต่อเนื่องของค่าความร้อนจำเพาะที่อุณหภูมิวิกฤตในตัวนำยวดยิ่งอุณหภูมิสูงที่มีความหนาแน่นสถานะคงที่และที่ขึ้นกับพลังงานแบบ แวน โฮฟ ซิงกูลาริตี โดยการใช้ทฤษฎีตัวนำยวดยิ่งของ บาร์ดีน คูเปอร์ และชรีฟเฟอร์ (Bardeen, Cooper, and Schrieffer) โดยพิจารณาสภาพการจับคู่ของอิเล็กตรอนที่ไม่ขึ้นกับทิศทาง (s-wave) และที่ขึ้นกับทิศทาง (d-wave) สามารถหาสมการแสดงอัตราส่วนระหว่างค่าความไม่ต่อเนื่องของค่าความร้อนจำเพาะที่อุณหภูมิวิกฤต ($\Delta C(T_c)$) กับค่าความร้อนจำเพาะในสถานะปกติที่อุณหภูมิวิกฤต ($C_N(T_c)$) เป็นฟังก์ชันของ ความถี่เดอบาย อุณหภูมิวิกฤต และพลังงานเฟอร์มิ ซึ่งแสดงให้เห็นว่าอัตราส่วนดังกล่าวแตกต่างไปจากค่า 1.43 ที่คำนวณโดย BCS

จุฬาลงกรณ์มหาวิทยาลัย

ภาควิชา ฟิสิกส์	ลายมือชื่อนิสิต .....
สาขาวิชา ฟิสิกส์	ลายมือชื่ออาจารย์ที่ปรึกษา .....
ปีการศึกษา 2542	ลายมือชื่ออาจารย์ที่ปรึกษาร่วม .....

4072424423 : MAJOR PHYSICS

KEY WORD: SPECIFIC HEAT JUMP / S-WAVE / D-WAVE / PAIRING STATES / VAN HOVE SINGULARITY

SUCHAT KASKAMALAS : ELECTRONIC SPECIFIC HEAT DISCONTINUITY AT CRITICAL TEMPERATURE OF HIGH-T_c SUPERCONDUCTORS. THESIS ADVISOR : PROF. VIRULH SA-YAKANIT. F.D., THESIS COADVISOR : PROF. SUTHAT YOKSAN. Ph.D., 70 pp. ISBN 974-333-903-5.

The purpose of this thesis is to investigate the specific heat jump at the critical temperature of high-T_c superconductor having the constant and the Van Hove Singularity density of states. By using the theory of Bardeen, Cooper, and Schrieffer (BCS) and considering the pairing states to be isotropic s-wave and anisotropic d-wave, we calculate the ratio between the jump in the specific heat and the normal phase specific heat at the critical temperature as a function of the Debye frequency, the critical temperature, and the Fermi energy, the results show significant deviations from the BCS value of 1.43.

จุฬาลงกรณ์มหาวิทยาลัย

ภาควิชา ฟิสิกส์	ลายมือชื่อนิสิต .....
สาขาวิชา ฟิสิกส์	ลายมือชื่ออาจารย์ที่ปรึกษา .....
ปีการศึกษา 2542	ลายมือชื่ออาจารย์ที่ปรึกษาร่วม .....

หอสมุดกลาง สถาบันวิทยบริการ จุฬาลงกรณ์มหาวิทยาลัย

Acknowledgment

The author wishes to express grateful thanks to his thesis advisor, Prof. Virulh Sa-yakanit for his encouragement and guidance throughout the course of investigation.

He would like to express his gratitude to his co-advisor, Prof. Suthat Yoksan for his advice, encouragement and helps in various ways.

He also would like to thank the thesis committee, Assoc. Prof. Kitt Visoottiviseth, Dr. Pornthep Nisamaneephong, and Assoc. Prof. Wichit Sritrakool for their reading and criticizing of the manuscipt.

จุฬาลงกรณ์มหาวิทยาลัย

Contents

	Page
Abstract in Thai	iv
Abstract in English	v
Acknowledgment	vi
List of Tables	ix
List of Figures	x
Chapter 1 Introduction	1
Chapter 2 BCS Theory	6
2.1 Introduction	6
2.2 Cooper pairs	8
2.3 Formulation of the BCS theory	11
2.4 Thermodynamic functions	18
Chapter 3 High-T_c Van Hove Superconductors	25
3.1 Introduction	25
3.2 The discovery of high-T_c superconductors	27
3.3 Structures of cuprate superconductors	30
3.4 Tetragonal-orthorhombic transition and twinning	35
3.5 The Van Hove scenario	36

3.6 Van Hove singularity in the density of states 39

Chapter 4 Specific heat jump at T_c of high-T_c superconductors 44

4.1 Introduction 44

4.2 Temperature dependence of the order parameter and specific heat jump at T_c 47

4.3 Effect of the constant density of states 51

4.4 Effect of the Van Hove singularity density of states 55

Chapter 5 Discussion and conclusions 60

References 65

Curriculum Vitae 70

จุฬาลงกรณ์มหาวิทยาลัย

List of Tables

Table Page

3.1 The best known cuprate superconductors, showing the stacking of planes in the c direction 28

จุฬาลงกรณ์มหาวิทยาลัย

List of Figures

Figure Page

2.1 Critical magnetic field of a superconductor 20

2.2 Plot of the ratio of the electronic specific heat to γT_c vs. T/T_c ... 23

3.1 Maximum superconducting critical temperature T_c vs. date 29

3.2 The Perovskite structure ABX_3 and stacking of planes in YBCO .. 34

3.3 Orthorhombic-tetragonal transition in YBCO, simulation of the tweed pattern of microtwins generated by the transition in YBCO at low temperatures, and corresponding simulation of the stripe pattern which appears on annealing 34

3.4 Idealized Fermi surface in Van Hove scenario 38

3.5 The singularities density of states 43

4.1 The jumps in specific heat for the constant density of states at the Fermi level 54

4.2 The normalized electronic specific heat jump of a Van Hove superconductor 59

Chapter 1

Introduction

The 1986 discovery of a class of copper oxide alloys that are able to conduct electricity with zero resistance at high temperatures began an exciting race to find new superconductors (Bednorz and Müller, 1986). The mercury-based cuprates now exhibit superconducting transition temperatures T_c that are halfway to room temperature, a record that is five times higher than previously believed limits (Schilling et al., 1993).

Bednorz and Müller began their inventive quest by synthesizing oxides that are usually considered closer to the realm of insulators rather than to the conventional metal category. They found that $La_{2-x}Ba_xCuO_4$ is superconducting up to 35 K for a rather limited range of compositions, for which an anomalous metallic character of the electron motion is indicated by the optical conductivity and various other transport properties at high temperatures (Bednorz and Müller, 1988).

Experimental evidences indicate that in high temperature superconductors electrons (or holes) conduct current primarily along planes determined by the copper-oxide atom layers in the cuprate structure, whereas the larger spacing between layers creates a barrier to conduction perpendicular

to these planes. A mysterious damping of the charge carriers in these high-T_c cuprates distinguishes them from other anisotropic materials. The peculiar linear frequency variation of the observed damping has led some to question the existence of a Fermi surface in the cuprates, while others have proposed that the source of the damping provides clues to the superconducting mechanism in these strange alloys.

Chu's group (Wu et. al., 1987) found that applied pressure elevates T_c in the La-based cuprate and thus reasoned that rare earth atoms with a smaller ionic radius may exert a desired chemical pressure in the cuprate lattice. They discovered the superconductor $YBa_2Cu_3O_7$ with a transition temperature near 90 K, which raised hoped for technological applications since these materials could be cooled with liquid nitrogen refrigerants instead of the more costly and cumbersome helium facilities that are used with standard superconducting magnets.

Escalating optimism was encouraged by discoveries of T_c = 125 K in thallium-based cuprates (Hermann and Yakhmi, 1994) and the 130 K (Schilling et al., 1993) in Hg-1223. Application of pressure (Chu et al., 1993) to Hg-1223 pushed the current record (T_c=165K) halfway to room temperature.

Since many high-T_c oxide superconductors are found to contain a number of layers of CuO_2. In order to understand the origin of high critical temperatures in these cuprates. Labbe and Bok (Labbe and Bok, 1987)

stressed the important role played by the CuO_2 planes by pointing out that the CuO_2 planes are sometimes well separated, therefore the electronic properties of these oxides are expected to show a two-dimensional behaviors rather than a three-dimensional one. The electronic structure of a 2D-lattice on account of its topological necessity reveals the occurrence of at least one Van Hove Singularity in the form of a saddle point which, in turn, leads to a logarithmic peak in the electronic density of states. Recent high-resolution angle-resolved photoemission spectroscopy measurements on high-T_c superconductors (Dessau et al., 1993, Gofron et al., 1994, and Ma et al., 1995) have identified the presence of saddle points in the band structure of these materials and these saddle points are shown to correspond to logarithmic Van Hove Singularity (VHS) in the density of states. The influences of VHS on several properties of cuprate superconductors have been studied (Newns et al., 1992, 1994, and Houssa et al., 1997).

Specific heat is an important property of a superconductor. It can inform us about the nature of phase transition and the symmetry of the pairing state (Gopal, 1996), (Junod, 1990). The jump in the specific heat, ΔC, at the critical temperature provides a relative measure of the superconducting fraction that undergoes the superconducting transition. In BCS theory the ratio $\Delta C(T_c)/C_N(T_c)$, is a universal constant, 1.43, here C_N is the normal state specific heat. In many high temperature cuprate superconductors this ratio has been found to be greater than the BCS value (Gopal, 1996), (Junod, 1990).

The explanation of this discrepancy has been attributed to the logarithmic VHS in the normal state density of states with s-wave order parameter (Tsuei et al., 1992, Gama Goicochea, 1994) and also with d-wave order parameter (Dorbolo et al., 1996, Dorbolo, 1997). Sarkar and Das (Sarkar and Das, 1996) studied the specific heat jump of s-wave cuprates and found that an extended VHS can account for some of the experimental results reasonably well. In their investigation of the specific heat jump, Newns et al. (Newns et al., 1995) showed that the d-wave version of the Van Hove scenario at the BCS level of approximation is viable. Recently Dagotto et al. (Dagotto et al., 1995) proposed a theoretical model including both the VHS and antiferromagnetic fluctuation effects. Their model explains many features of high-T_c materials and predicts a gap parameter of $d_{x^2-y^2}$ –wave type (Tsuei and Kirtley, 1997).

Within the BCS framework, the specific heat jump is usually calculated from the temperature derivative of the square of the gap parameter and the reduced gap ratio (R), by defining $A^2 = -d[\Delta(T)/\Delta(0)]^2/d(T/T_c)$ and $B^2 = [\Delta(0)/T_c]^2$, here $\Delta(T)$ is the temperature-dependent energy gap function, Tsuei et al. obtain $A=1.74$, $B=1.76$ (Tsuei et al., 1992), (Gama Goicochea, 1994), (Sarkar and Das, 1996). As is well known these quantities having such values when the condition $\omega_D/T_c \to \infty$ is considered. In conventional superconductors this restriction is valid because the cutoff energy ω_D is much

หอสมุดกลาง สถาบันวิทยบริการ
จุฬาลงกรณ์มหาวิทยาลัย

greater than T_c. With the discovery of high temperature oxides the Debye cutoff ω_D is not that much greater than T_c, the dimensionless ratio ω_D / T_c is therefore finite. Hence new calculations of A and B are needed (Krunavakarn et al., 1998), (Pakokthom et al., 1998).

It is therefore of great interest to obtain exact analytical expression for $\Delta C(T_c)/C_N(T_c)$ without making any approximation concerning ω_D / T_c, to know what the BCS Theory predicts for A, B and $\Delta C(T_c)/C_N(T_c)$ when ω_D / T_c is beyond its restricted value. The purpose of this research is to investigate the specific heat jump of isotropic s-wave and anisotropic d-wave superconductors within the BCS framework for a constant density of states and for a VHS density of states.

We review the BCS theory in Chapter 2, and some theories of high-T_c superconductors, especially the Van Hove superconductors, in Chapter 3. In Chapter 4, we present our calculations for the specific heat jump ($\Delta C(T_c)/C_N(T_c)$) of isotropic s- wave and anisotropic d- wave superconductors. Starting with the BCS gap equation, we derive a formal but completely general formula for the temperature dependence of the order parameter and the normalized specific heat jump. The effects of the constant and VHS density of states on the specific heat difference are presented analytically and graphically. Finally, discussions and conclusions are drawn in Chapter 5.

Chapter 2

The BCS Theory

2.1 Introduction

The theory of superconductivity developed by Bardeen, Cooper, and Schrieffer (BCS) (Bardeen et al., 1957) was founded on a number of assumptions concerning the causes of superconductivity which, on the basis of theory and experiment, were generally agreed. Experimental evidence pointed to the fact that in the transition of a metal to the superconductive state the lattice and its properties were essentially unchanged, whereas some of the properties of the conduction electrons were changed radically. In the first instance, at least, it was reasonable to assume that transition was caused by a change in the state of the electrons alone.

The way to understand the phenomenon of superconductivity is due to Fröhlich (Fröhlich, 1953) who proposed the interaction which is now generally believed to give rise to superconductivity in most, if not all, known superconductors. This interaction between the electrons arises as a result of the interaction of the electrons with the possible vibrations of the lattice (phonon). Its

significance in causing superconductivity is confirmed by the dependence of the critical temperature of superconductors on the isotopic mass of the lattice, a dependence which was established (Maxwell, 1950, Reynolds et al., 1950) independently.

Phonons are collective excitations of the lattice. The vibrational state of the lattice is characterized by the number of phonons in the individual oscillator states defined by the wave vector $\mathbf{q}$ and the branch j of the dispersion spectrum $\omega_j(\mathbf{q})$.

This interaction between the electrons which is mediated by the phonons can be written as (Madelung, 1978)

$$\begin{aligned} V_{\mathbf{kq}} &= |M_{\mathbf{q}}|^2 \left[\frac{1}{E(\mathbf{k}) - E(\mathbf{k}+\mathbf{q}) - \hbar\omega_{\mathbf{q}}} - \frac{1}{E(\mathbf{k}) - E(\mathbf{k}+\mathbf{q}) + \hbar\omega_{\mathbf{q}}} \right] \\ &= \frac{2|M_{\mathbf{q}}|^2 \hbar\omega_{\mathbf{q}}}{[E(\mathbf{k}+\mathbf{q}) - E(\mathbf{k})]^2 - (\hbar\omega_{\mathbf{q}})^2}. \end{aligned} \tag{2.1}$$

here, $M_{\mathbf{q}}$ is the coupling strength of an electron-phonon interaction matrix element, $\omega_{\mathbf{q}}$ is the phonon frequency, and $E(\mathbf{k})$ is the excitation energy.

The basic electron-phonon interaction process is the annihilation (absorption) or creation (emission) of a phonon ($\mathbf{q}$, j) with simultaneous change of the electron state from $|\mathbf{k},\sigma\rangle$ to $|\mathbf{k} \pm \mathbf{q},\sigma\rangle$.

In the following sections we shall study the interaction more closely. It will emerge that, with particular assumptions, an attractive effective interaction leads

to a correlation of the electrons, which results in a reduction in energy of the ground state. The correlation takes place predominantly in pair between electrons of opposite spin and opposite wave vector (Cooper pairs). In Section 2.2 we shall look at individual Cooper pairs, and in Section 2.3 we shall present formulation of the BCS theory. Finally in the Section 2.4 we shall find the thermodynamic functions of the superconductive state.

2.2 Cooper Pairs

Cooper (Cooper, 1956) presented the basic idea that even a weak attraction can bind pairs of electrons into a bound state. To grasp the significant aspects of the new interaction, we consider an idealized case: a noninteracting electron gas fills the Fermi sphere in $\mathbf{k}$-space. All the states below E_F are occupied, and all above it empty. Into this system we introduce two electrons $[\mathbf{k}_1, E(\mathbf{k}_1)]$ and $[\mathbf{k}_2, E(\mathbf{k}_2)]$. We take the positive part of $V_{\mathbf{kq}}$ in Eq.(2.1) as the interaction between these two electrons. Interaction processes involving phonon exchange will therefore only occur for $|E(\mathbf{k}+\mathbf{q}) - E(\mathbf{k})| \le \hbar\omega_{\mathbf{q}}$.

We construct the wave function for the electron pair by the application of two creation operators to the ground state $|G\rangle$ (filled Fermi sphere), summing over all possible $\mathbf{k}_1$ and $\mathbf{k}_2$ $(k_i > k_F)$ and over the electron spins

$$\psi_{12} = \sum_{\mathbf{k}_1\mathbf{k}_2\sigma_1\sigma_2} a_{\sigma_1\sigma_2}(\mathbf{k}_1,\mathbf{k}_2)\, c^{+}_{\mathbf{k}_1\sigma_1} c^{+}_{\mathbf{k}_2\sigma_2} |G\rangle \qquad (2.2)$$

where $\mathbf{k}_i, \sigma_i$ are the wave vectors and the spins of the electron, respectively. $a_{\sigma_1\sigma_2}(\mathbf{k}_1,\mathbf{k}_2)$ denotes the probability amplitude in finding the particle at the wave vectors $\mathbf{k}_1$ and $\mathbf{k}_2$ with σ_1 and σ_2, simultaneously and $c^+_{\mathbf{k}_i\sigma_i}$ represents the electron creation operator. The sum over the wave vectors is subjected to the condition $\mathbf{k} = \mathbf{k}_1 + \mathbf{k}_2$ = constant. If we choose $\mathbf{k} = 0$ the interaction energy of the electrons pair will be largest. Thus in this case $\mathbf{k}_1 = -\mathbf{k}_2 = \mathbf{k}$ and we assume that both electron spins are antiparallel i.e., $\sigma_1 = -\sigma_2 = \sigma$, then Eq.(2.2) becomes

$$\psi_{12} = \sum_{\mathbf{k}} a(\mathbf{k})\, c^+_{\mathbf{k},\sigma} c^+_{-\mathbf{k},-\sigma} |G\rangle . \tag{2.3}$$

The next task is to calculate the energy of the electron pair by using the wave function in Eq.(2.3). We take the interaction between electrons $V_{\mathbf{kq}}$ to be constant in the range of the attractive interaction and vanish elsewhere:

$$V_{\mathbf{kq}} = \begin{cases} -V, & |E(\mathbf{k}+\mathbf{q}) - E(\mathbf{k})| \le \hbar\omega_{\mathbf{q}} \\ 0, & \text{otherwise.} \end{cases} \tag{2.4}$$

The Hamiltonian will take the form

$$H = \sum_{\mathbf{k}\sigma} E(\mathbf{k}) c^+_{\mathbf{k},\sigma} c_{\mathbf{k},\sigma} - \frac{V}{2} \sum_{\mathbf{k}\mathbf{q}\sigma} c^+_{\mathbf{k}+\mathbf{q},\sigma} c^+_{-\mathbf{k}-\mathbf{q},-\sigma} c_{-\mathbf{k},-\sigma} c_{\mathbf{k}\sigma} . \tag{2.5}$$

For $\omega_{\mathbf{q}}$ we choose a characteristic frequency of the phonon spectrum, e.g., the Debye frequency ω_D, as the maximum value of $\omega_{\mathbf{q}}$ in the Debye approximation.

We then find

$$E = \langle \psi | H | \psi \rangle = 2\sum_{\mathbf{k}} E(\mathbf{k}) |a(\mathbf{k})|^2 - V\sum_{\mathbf{kq}} a^*(\mathbf{k}+\mathbf{q}) a(\mathbf{k}) . \tag{2.6}$$

We determine the $a(\mathbf{k})$ by varying E subject to the condition $\sum_{\mathbf{k}} |a(\mathbf{k})|^2 = 1$

$$\frac{\partial}{\partial a^*_{\mathbf{k}'}} \left[E - \lambda \sum_{\mathbf{k}''} |a(\mathbf{k}'')|^2 \right] = 2E(\mathbf{k}') a(\mathbf{k}') - V\sum_{\mathbf{q}} a(\mathbf{k}'-\mathbf{q}) - \lambda a(\mathbf{k}') = 0 \tag{2.7}$$

or

$$[2E(\mathbf{k}) - \lambda] a(\mathbf{k}) = V\sum_{\mathbf{k}'} a(\mathbf{k}') . \tag{2.8}$$

We satisfy the restriction on the interaction by taking V only nonzero for energies in the range E_F to $E_F \pm \hbar\omega_D$. The same is also true for the $a(\mathbf{k})$, and the sum in Eq.(2.8) runs over a finite number of $\mathbf{k}'$. Calling this sum C we find

$$a(\mathbf{k}) = \frac{VC}{2E(\mathbf{k}) - \lambda}, \qquad \sum_{\mathbf{k}} a(\mathbf{k}) = C = \sum_{E(\mathbf{k})} \frac{VC}{2E(\mathbf{k}) - \lambda} . \tag{2.9}$$

The sum here runs over all states between E_F and $E_F \pm \hbar\omega_D$.

The final step is to return to Eq. (2.8). If we take the complex conjugate of this equation, multiply by $a(\mathbf{k})$, and sum over $\mathbf{k}$, an equation follows which agrees with Eq.(2.6) if one puts $\lambda = E$. Thus we have determined the Lagrange parameter and can write the second equation of (2.9) in the following form

$$1 = \sum_{E(\mathbf{k})} \frac{V}{2E(\mathbf{k}) - E} = V \int_{E_F}^{E_F + \hbar\omega_D} \frac{N(x)dx}{2x - E} . \tag{2.10}$$

In transforming the sum into an integration, the density of states $N(E)$ has been introduced. In view of the narrow range of integration, $E_F >> \omega_D$, we put $N(E) \approx N(E_F)$. The integral can be evaluated and one obtains

$$E = 2E_F - \frac{2\hbar\omega_D \exp[-2/N(E_F)V]}{1-\exp[-2/N(E_F)V]} \approx 2E_F - 2\hbar\omega_D \exp[-2/N(E_F)V]. \qquad (2.11)$$

This energy is correct when V is small (weak interaction, $N(E_F)V << 1$). Eq.(2.11) shows the presence of the bound state of the electron pair which is called the Cooper pair. The context of the Cooper's idea leads us to explain the ground state of the superconducting electron gas.

2.3 Formulation of the BCS Theory

Bardeen, Cooper, and Schrieffer (BCS) (Bardeen et al., 1957) developed further the Cooper's idea, they suggested that superconductivity arises from the presence of the Cooper pair mediated by the electron-phonon interaction. The ground state of the superconducting state with no supercurrent at the absolute zero of temperature may be written as

$$|BCS\rangle = \prod_{\mathbf{k}} \left(u_{\mathbf{k}} + v_{\mathbf{k}} c^{+}_{\mathbf{k}\uparrow} c^{+}_{-\mathbf{k}\downarrow}\right)|0\rangle \qquad (2.12)$$

In this state the electrons are created in $(\mathbf{k}\uparrow, -\mathbf{k}\downarrow)$ pairs, all having the zero pair momentum and also the zero total spin. The parameter $u_{\mathbf{k}}$ and $v_{\mathbf{k}}$ are real with the normalization condition $u_{\mathbf{k}}^2 + v_{\mathbf{k}}^2 = 1$. $u_{\mathbf{k}}^2$ is the probability that the momentum pair

state is empty while v_k^2 the probability that it is occupied. BCS started from the wave function and found the coefficients u_k and v_k from the variational principle. The model Hamiltonian proposed by BCS is given by

$$H = \sum_{k\sigma} \varepsilon(\mathbf{k}) c_{k\sigma}^{+} c_{k\sigma} + \sum_{kk'} V_{kk'} c_{k\uparrow}^{+} c_{-k\downarrow}^{+} c_{-k'\downarrow} c_{k'\uparrow} \tag{2.13}$$

where $\varepsilon(\mathbf{k})$ is the energy of a conduction electron with respect to the chemical potential, μ. The creation and destruction operators for electrons of wave vector $\mathbf{k}$ and z component of spin σ (up or down) are denote by $c_{k\sigma}^{+}$ and $c_{k\sigma}$, respectively. The interaction matrix element $V_{kk'}$ represents the scattering of one pair of states $(\mathbf{k}\uparrow,-\mathbf{k}\downarrow)$ into another pair of states $(\mathbf{k}'\uparrow,-\mathbf{k}'\downarrow)$. The solution of the Hamiltonian cannot be obtained by perturbation theory since the quasi particle picture of the normal state is insufficient to provide the superconducting phase. The important feature of the quasi particle picture is that the interaction between the quasi particles is neglected and absorbed into the effective mass of electrons.

Since the interaction term assumes that such electron pairs act as units, the ground state will be some coherent superposition of many-body states in which the states $(\mathbf{k}\uparrow,-\mathbf{k}\downarrow)$ are occupied or unoccupied in pairs. This means that the operator $c_{-k\downarrow}c_{k\uparrow}$ is equal to the thermal average $< c_{-k\downarrow}c_{k\uparrow} >$ and the fluctuation

term, $c_{-k\downarrow}c_{k\uparrow} - < c_{-k\downarrow}c_{k\uparrow} >$, should be negligible. In general, the pair operators $c_{-k\downarrow}c_{k\uparrow}$ can be written in the form

$$c_{-k\downarrow}c_{k\uparrow} =< c_{-k\downarrow}c_{k\uparrow} > +(c_{-k\downarrow}c_{k\uparrow} - < c_{-k\downarrow}c_{k\uparrow} >) \tag{2.14}$$

The expectation value of this operator is now determined. A gap parameter is defined by

$$\Delta_{k'} = -\sum_{k} V_{kk'} < c_{-k\downarrow}c_{k\uparrow} > \tag{2.15}$$

Δ_k is a new quantity and may be thought of as being like as internal field, it expresses the influence of the mixed occupation in all the other $(\mathbf{k}'\uparrow,-\mathbf{k}'\downarrow)$ pairs of the $(\mathbf{k}\uparrow,-\mathbf{k}\downarrow)$ pair through the attractive matrix elements. Using Eqs. (2.14) and (2.15), the model Hamiltonian becomes

$$H = \sum_{k\sigma} \varepsilon(\mathbf{k}) c^{+}_{k\sigma} c_{k\sigma} + \sum_{k} (\Delta_k c^{+}_{k\uparrow} c^{+}_{-k\downarrow} + \Delta^{*}_k c_{-k\downarrow} c_{k\uparrow} - \Delta^{*}_k < c_{-k\downarrow} c_{k\uparrow} >) \tag{2.16}$$

Since this Hamiltonian is now quadratic, it can be diagonalized by the canonical transformation

$$c_{k\uparrow} = u_k a_{k1} + v^{*}_k a^{+}_{k2}$$

$$c^{+}_{-k\downarrow} = -v_k a_{k1} + u^{*}_k a^{+}_{k2} \tag{2.17}$$

where the new operators a_{k1} and a_{k2} are Fermion annihilation operators. The parameters u_k and v_k are chosen such that the coefficients of the mixed terms such as $c^{+}_{k1}c^{+}_{k2}$ in the Hamiltonian vanish. This can be satisfied if

$$2\varepsilon(\mathbf{k})u_k v_k + \Delta_k v_k^2 - \Delta_k^* u_k^2 = 0 . \tag{2.18}$$

From the canonical transformation, the important property is that the anticommutation relations between the a's being the same as those between the c's, and the constraint is that

$$|u_k|^2 + |v_k|^2 = 1 . \tag{2.19}$$

Since there is no external field associated with the system, the parameter u_k and v_k are real and if we also introduce the quantity

$$E_k = \sqrt{\varepsilon^2(\mathbf{k}) + |\Delta_k|^2} . \tag{2.20}$$

We thus obtain the coefficients u_k, v_k from Eqs. (2.18) and (2.19) as

$$u_k^2 = \frac{1}{2}\left(1 + \frac{\varepsilon(\mathbf{k})}{E_k}\right),$$

$$v_k^2 = \frac{1}{2}\left(1 - \frac{\varepsilon(\mathbf{k})}{E_k}\right). \tag{2.21}$$

The model Hamiltonian is now diagonalized, the result is

$$H = \sum_k E_k (a_{k1}^+ a_{k1} + a_{k2}^+ a_{k2}) + \sum_k (\varepsilon(\mathbf{k}) - E_k + \Delta_k^+ < c_{-k\downarrow} c_{k\uparrow} >) \tag{2.22}$$

this Hamiltonian contains the average of the operators $c_{-k\downarrow} c_{k\uparrow}$. The expectation value of this operator is given by

$$\begin{aligned} < c_{-k\downarrow} c_{k\uparrow} > &= \mathrm{Tr}[\exp(-\beta H) c_{-k\downarrow} c_{k\uparrow}] / \mathrm{Tr}[\exp(-\beta H)] \\ &= u_k v_k^* \mathrm{Tr}[\exp(-\beta H)(-a_{k1}^+ a_{k1} + a_{k2} a_{k2}^+)] / \mathrm{Tr}[\exp(-\beta H)] \\ &= u_k v_k^* [1 - 2 f(E_k)] \end{aligned} \tag{2.23}$$

where Tr represents the trace in the occupation number Hilbert space, β is the inverse of temperature T and $f(E)$ is the Fermi function,

$$f(E) = \frac{1}{\exp(\beta E) + 1}. \tag{2.24}$$

Using Eqs. (2.15), (2.21), and (2.23) the gap parameter is determined to be

$$\Delta_{\mathbf{k}} = -\sum_{\mathbf{k}'} V_{\mathbf{k}\mathbf{k}'} \frac{\Delta_{\mathbf{k}'}}{2E_{\mathbf{k}'}} \tanh(E_{\mathbf{k}'}/2T). \tag{2.25}$$

This equation is non-linear because $E_{\mathbf{k}}$ depends on $\Delta_{\mathbf{k}}$ and it can be solved by the numerically method or the approximation one. In order to determine the critical temperature T_c, we put $E_{\mathbf{k}} = \varepsilon(\mathbf{k})$ in Eq. (2.25) and obtain

$$\Delta_{\mathbf{k}} = -\sum_{\mathbf{k}'} V_{\mathbf{k}\mathbf{k}'} \frac{\Delta_{\mathbf{k}'}}{2\varepsilon(\mathbf{k}')} \tanh(\varepsilon(\mathbf{k}')/2T_c) \tag{2.26}$$

where the pair-excitation spectrum is taken at temperature T_c. To solve Eq.(2.26) we assume a constant gap for $|\varepsilon(\mathbf{k})| \le \omega_D$, i.e. $\Delta_{\mathbf{k}} = \Delta$, we, furthermore, assume the approximation for $V_{\mathbf{k}\mathbf{k}'}$ as

$$V_{\mathbf{k}\mathbf{k}'} = \begin{cases} -V, & |\varepsilon(\mathbf{k})|, |\varepsilon(\mathbf{k}')| \le \omega_D \\ 0, & \text{otherwise} \end{cases} \tag{2.27}$$

This model is valid only for the weakly coupled superconductors (e.g. aluminium and tin) for which $N(0)V$ is very much less than unity, and not for strongly coupled superconductors (e.g., lead and mercury). By virtue of this approximation, the equation for T_c is determined from the equation

$$\frac{1}{N(0)V} = \int_0^{\omega_D} \frac{d\varepsilon}{\varepsilon} \tanh(\varepsilon / 2T_c) \tag{2.28}$$

Introducing the dimensionless variable $x = \varepsilon / 2T_c$, with the integration by parts, we have

$$\begin{aligned} \frac{1}{N(0)V} &= \ln(\frac{\omega_D}{2T_c}) \tanh(\frac{\omega_D}{2T_c}) - \int_0^{\omega_D / 2T_c} dx \ln x \operatorname{sech}^2 x \\ &\cong \ln(\frac{2e^{\gamma}\omega_D}{\pi T_c}) \end{aligned} \tag{2.29}$$

where the upper limit of the last integral is extended to infinity and it value is equal to $-\ln(4e^{\gamma} / \pi)$, with the Euler constant, $\gamma = 0.5772$. Thus the equation for T_c is given by

$$T_c = 1.13\omega_D \exp(-\frac{1}{N(0)V}). \tag{2.30}$$

To find the solution for the gap parameter Δ_k, we consider only the interaction having the form of Eq. (2.27) and consequently the gap parameter satisfies the equation

$$\frac{1}{N(0)V} = \int_0^{\omega_D} \frac{d\varepsilon}{E} \tanh(E / 2T) \tag{2.31}$$

where

$$E = \sqrt{\varepsilon^2 + \Delta^2}\ . \tag{2.32}$$

At the absolute zero of temperature Eq.(2.31) becomes

$$\frac{1}{N(0)V} = \int_0^{\omega_D} \frac{d\varepsilon}{\sqrt{\varepsilon^2 + \Delta^2(0)}} \tag{2.33}$$
$$= \sinh^{-1}\left(\frac{\omega_D}{\Delta(0)}\right)$$

In the weak coupling limit $\omega_D >> \Delta(0)$, we can approximate $\sinh^{-1} x \cong \ln 2x$ for $x >> 1$ in Eq.(2.33). Hence, the solution for the gap parameter at the absolute zero of temperature is

$$\Delta(0) = 2\omega_D \exp\left(-\frac{1}{N(0)V}\right). \tag{2.34}$$

Combining Eqs. (2.30) and (2.34), the ratio of the gap parameter at the absolute zero temperature to the critical temperature is

$$\Delta(0)/T_c = 1.76, \tag{2.35}$$

which is a universal constant independent of the particular material.

2.4 Thermodynamic Functions

2.4.1 Isotropic Superconductors

We proceed to evaluate the sum-over-states, or partition function Z, and from that the other thermodynamic functions of the superconductive state. By definition

$$\begin{aligned} Z &= \mathrm{Tr}\exp(-\beta H) \\ &= \prod_{\mathbf{k}} \mathrm{Tr}\exp(-\beta E_k a_{k1}^{+} a_{k1})\, \mathrm{Tr}\exp(-\beta E_k a_{k2}^{+} a_{k2}) \\ &\qquad \times \exp\left\{-\beta(\varepsilon(\mathbf{k}) - E_k + \Delta_k^2[1-2f(E_k)]/2E_k)\right\} \end{aligned} \tag{2.36}$$

The traces are evaluated to yield

$$Z = \prod_{\mathbf{k}} [1 + \exp(-\beta E_{\mathbf{k}})]^2 \exp\left\{ -\beta \sum_{\mathbf{k}} (\varepsilon(\mathbf{k}) - E_{\mathbf{k}} + \Delta_{\mathbf{k}}^2 [1 - 2f(E_{\mathbf{k}})]/2E_{\mathbf{k}}) \right\} \qquad (2.37)$$

From this one calculates the thermodynamic potential for the electrons,

$$\begin{aligned} \Omega_s &= -\frac{1}{\beta} \ln Z \\ &= -\frac{2}{\beta} \sum_{\mathbf{k}} \ln[1 + \exp(-\beta E_{\mathbf{k}})] + \sum_{\mathbf{k}} \left\{ \varepsilon(\mathbf{k}) - E_{\mathbf{k}} + \Delta_{\mathbf{k}}^2 [1 - 2f(E_{\mathbf{k}})]/2E_{\mathbf{k}} \right\} \end{aligned} \qquad (2.38)$$

This thermodynamic potential can be related to the critical magnetic field of the superconductor. From general thermodynamic arguments, the critical magnetic field at a certain temperature can be related to the difference in the Gibbs free energy of the superconductor in the normal and superconductive states. Since this free energy change comes from the electrons and since the changes in volume and chemical potential of the electrons in the transition are negligible, the difference in the Gibbs free energy is equal to the difference in the thermodynamic potentials of the electrons. Hence we have

$$\nu H_c^2 / 8\pi = \Omega_n - \Omega_s \qquad (2.39)$$

here ν is the volume, Ω_s is given by Eq.(2.38), and Ω_n is given by Eq.(2.38) with Δ put equal to zero.

For a general temperature, Ω_s cannot be calculated analytically. It can, however, be evaluated analytically for the absolute zero of temperature. For this case

$$\Omega_s = 2N(0)\int_0^{\hbar\omega_D} d\varepsilon\left(\varepsilon - E + \Delta^2/2E\right) \tag{2.40}$$

and, in the limit of $\hbar\omega_D$ very much greater than Δ

$$\Omega_s = -\frac{1}{2}N(0)\Delta^2 . \tag{2.41}$$

Hence the critical magnetic field at the absolute zero, $H_c(0)$, is given by

$$H_c^2(0)/8\pi = \frac{1}{2}N(0)\Delta^2 \tag{2.42}$$

The three quantities $H_c(0)$, $N(0)$, $\Delta(0)$ can all be measured, hence Eq. (2.42) can be put to test. Near the absolute zero of temperature one can show that

$$H_c(T)/H_c(0) \approx 1 - 1.06(T/T_c)^2 \tag{2.43}$$

Near T_c the thermodynamic potential can be evaluated (Mühlschlegel, 1959) to give

$$H_c(T)/H_c(0) = e^{\gamma}\left[\frac{8}{7\varsigma(3)}\right]^{1/2}\left(1 - \frac{T}{T_c}\right) \tag{2.44}$$

where $\gamma = 0.5772$, and $\varsigma(x)$ is the Riemann zeta function. Hence

$$H_c(T)/H_c(0) \approx 1.74\left(1 - \frac{T}{T_c}\right). \tag{2.45}$$

Thus the slope of the critical field curve is finite at T_c, as it should be according to the thermodynamic relations.

At intermediate values of T, the critical magnetic field is calculated numerically. The result is so close to the empirical formula

$$H_c(T)/H_c(0) = 1-(T/T_c)^2 \tag{2.46}$$

that it is usual to plot the deviation from this result,

$$D(T) = \frac{H_c(T)}{H_c(0)} - \left[1-(T/T_c)^2\right] \tag{2.47}$$

This is shown in Fig.2.1, where $D(T)$ is plotted vs. T/T_c; it is another universal function. These calculations confirm that as long as we can find a solution of the integral equation with Δ not equal to zero, this solution provides a state with lower free energy than the trivial solution.

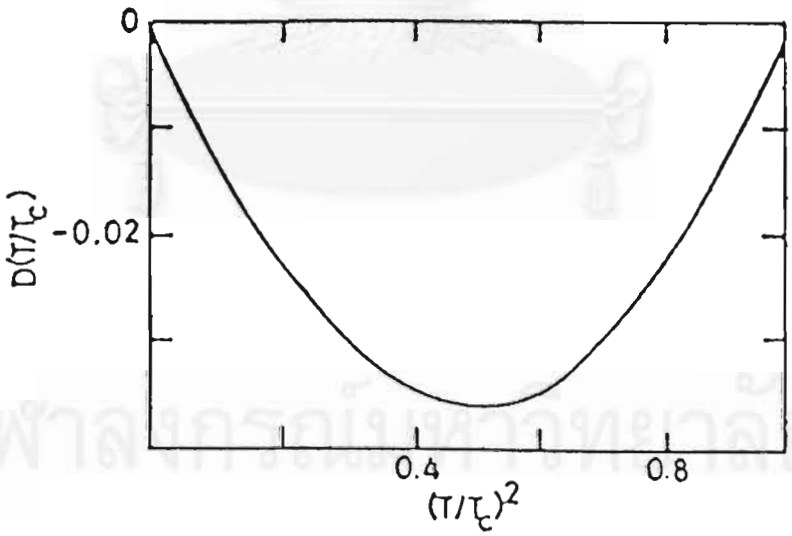

Figure 2.1: Critical magnetic field of a superconductor, illustrated by a plot of the deviation $D(T) = H_c(T)/H_c(0) - [1-(T/T_c)^2]$ from the old empirical rule versus $(T/T_c)^2$. Note the scale. (Parks, 1969)

หอสมุดกลาง สถาบันวิทยบริการ
จุฬาลงกรณ์มหาวิทยาลัย

The entropy of the electrons can be calculated from the formula

$$S_s = -\left(\frac{\partial \Omega}{\partial T}\right)_{\mu,v}. \tag{2.48}$$

Using the integral equation for Δ one finds

$$S_s = -2k_B \sum_k \{[1-f(E_k)]\ln[1-f(E_k)] + f(E_k)\ln f(E_k)\}. \tag{2.49}$$

This is the entropy of a gas of independent fermions, a result which is hardly surprising in view of the fact that the model Hamiltonian describes independent fermions.

Since the gap parameter tends to zero as T tends to T_c, the entropy is continuous at the critical temperature. There is, therefore, no latent heat evolved at the transition, and this result agrees with experiment. One can also see from Eq. (2.49) that as the temperature approaches the absolute zero, the entropy becomes exponentially small, being proportional to $\exp(-\Delta/kT)$.

The specific heat per unit volume of the electrons can be calculated from the formula

$$C_s = T\left(\frac{\partial S_s}{\partial T}\right)_{\mu,v}. \tag{2.50}$$

This is strictly the electronic specific heat at constant chemical potential, but since, when the number of particles is held fixed, the change of chemical potential

with temperature is negligible, we can ignore the difference between specific heats at constant chemical potential and specific heats at constant number of particles. This formula thus gives the measured electronic specific heat. Straightforward differentiation of Eq. (2.49) gives

$$\begin{aligned} C_s &= 2\sum_k E_k \frac{\partial f(E_k)}{\partial T} \\ &= -\frac{2}{T} N(0) \int_{-\infty}^{\infty} d\varepsilon \left(E^2 + \frac{\beta}{2}\frac{\partial \Delta^2}{\partial \beta} \right) \frac{\partial f}{\partial E} \end{aligned} \tag{2.51}$$

The curve of Δ^2 against temperature has a finite slope at the critical temperature. Hence the specific heat is not continuous there, and one has

$$\left. \frac{C_s - C_n}{C_n} \right|_{T_c} = \frac{3}{2\pi^2} \beta^3 \left. \frac{\partial \Delta^2}{\partial \beta} \right|_{T=T_c} = 1.43 \tag{2.52}$$

At lower temperatures the specific heat decreases rapidly, and because of the gap in the spectrum of excitation it becomes proportional to $\exp(-\Delta(0)/kT)$ at temperature below about $T_c/10$. A plot of the specific heat is shown in Fig.2.2 Again, according to the theory, C_s/C_n is a universal function of the reduced temperature. In any comparison of theory with experiment it must be remembered that it is the total specific heat which is usually measured, whereas, in this section, it is the electronic specific heat which is calculated. The comparison can, therefore, be made only if other contributions to the specific heat are first subtracted from the experimental results.

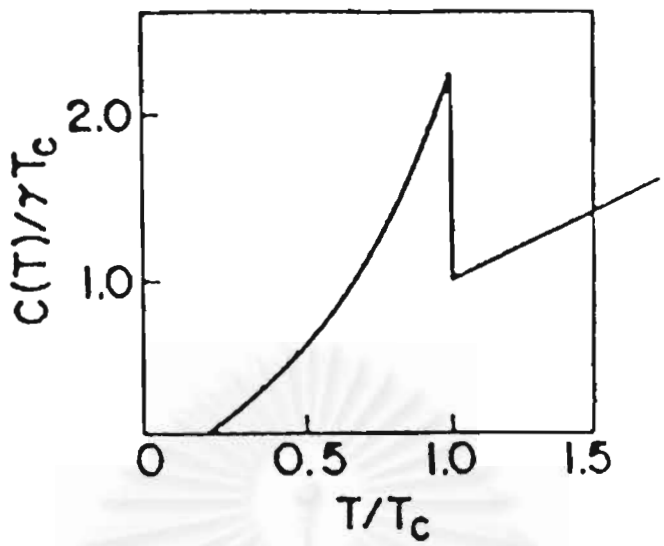

Figure 2.2: Plot of the ratio of the electronic specific heat to γT_c vs. T/T_c. (The electronic specific heat in the normal state is γT, γ is the Sommerfeld 's constant.) (Parks, 1969)

2.4.2 Anisotropic Superconductors

Some of the thermodynamic functions have been evaluated for anisotropic superconductors for which the gap parameter depends on angle (Pokrovskii and Ryvkin, 1962), (Geilikman and Kresin, 1963). Since such superconductors have to be described by more parameters than the $N(0)V$ of BCS, it is not possible to give the results in such a concise form. However, a number of inequalities have been proved (Pokrovskii and Ryvkin, 1962) and we give these inequalities for the sake

of a later comparison with experiment. From solutions of the integral equation (2.26) one finds that

$$2\Delta / kT_C \leq 3.53$$
$$\left.\frac{C_s - C_n}{C_n}\right|_{T_c} \leq 1.43 \qquad (2.53)$$

and near the absolute zero of temperature

$$H_c(T)/H_c(0) = 1 - \chi(T/T_c)^2 \qquad (2.54)$$

with $\chi \geq 1.06$. If the dynamic coupling between the electrons is taken into account, the first of these inequalities, even in an isotropic superconductor, can be broken (Wada, 1964), but the second still holds (Melik-Barkhudarov, 1965). If, however, the superconductor possesses overlapping conduction bands, it appears that even in an isotropic superconductor it is possible to break all three inequalities (Geilikman and Kresin, 1966).

จุฬาลงกรณ์มหาวิทยาลัย

Chapter 3

High-Temperature Van Hove Superconductors

3.1 Introduction

The discovery of superconductivity at ~30 K in the La-Ba-Cu-O system by Bednorz and Müller (Bednorz and Müller, 1986) ignited an explosion of interest in high-temperature superconductivity. These initial developments rapidly evolved into an intense worldwide research effort that still persists after more than a decade, fueled by the fact that high-temperature superconductivity constitutes an extremely important and challenging intellectual problem, and has enormous potential for technological applications. During the past decade of research on this subject, significant progress has been made on both the fundamental science and technological application fronts. For example, the symmetry of the superconducting order parameter and the identity of the superconducting electron pairing mechanism appear to be on the threshold of being established, and prototype superconducting wires that have current-carrying capacities in high magnetic fields that satisfy the requirements for applications are being developed.

Although the success of the discovery of the high-temperature cuprate lies on the experimental side but the understanding of their mechanism is also

unclear. Several theories have been proposed to describe the behavior of the high-T_c compounds. One- and three- band Hubbard models (Hubbard, 1963), as well as the t-J model (Zhang and Rice, 1988) are believed to represent the feature of the electronic behavior of the new materials. Unfortunately, most of the experimental data are not accurate enough to confirm the theories. The antiferromagnetic property of the normal state may be combined with the pairing ideas to describe the high-T_c superconductors. As in the spin bag theories (Schrieffer, Wen, Zhang, 1989), (Kampf and Schrieffer, 1990) which considers a hole moving in a background that has a spin density wave (SDW). A local distortion of the SDW order would create a spin bag and these bags attract to form Cooper pairs. In the antiferromagnetic Fermi-liquid theories Millis et al. (Millis, Monien, and Pines 1990) performed a study of the NMR spectra to extract a phenomenological model for the spin susceptibility. This model invokes a strong enhancement of the spin susceptibility near a nesting momentum at very low frequency. The interchange of magnons may produce the attractive force needed for the charge carriers (Miyake, Schmitt-Rink, and Varma, 1986). Among the Fermi-liquid-based theories one may include the Van Hove singularity scenario (Markiewicz, 1991), (Newns, Pattnaik, and Tsuei, 1991), and the nested Fermi liquid (Virosztek and Ruvalds, 1990).

In order to understand how the cuprate has the superconducting properties, the simplest way is to apply the BCS theory to the lattice taking

into account the properties of the crystal. Van Hove (Van Hove, 1953) stressed the crucial role played by the lattice topology. In the band structure of either electrons or phonons, Van Hove demonstrated that any non-analytic behavior in the density of states is caused by a change in the band topology. The singularity now known as Van Hove Singularities (VHS).

In superconducting materials, the role of a VHS is enhanced, because the density of states $N(E)$ can actually diverge at a VHS. In one-dimensional materials, the divergence is power law, $N(E) \propto \Delta E^{-1/2}$ where $\Delta E = E - E_{VHS}$. In two-dimensional materials, the density of states diverges logarithmically $N(E) \propto \ln(B/\Delta E)$, ΔE is the distance in energy from the VHS and B is the bandwidth.

In this chapter, we review the structures of cuprate and the properties of Van Hove superconductors.

3.2 The Discovery of High-T_c Superconductors

The dramatic increases in T_c that have been observed since 1986 are illustrated in Fig 3.1 where the maximum value of T_c is plotted versus date. The first of a new family of superconductors, now usually known as the high-T_c or cuprate superconductors, was discovered by Bednorz and and Müller (Bednorz and Müller, 1986). It was a calcium-doped lanthanum cuprate perovskite. When optimally doped to give the highest T_c, it had the formula $La_{1.85}Ca_{0.15}CuO_4$, with a T_c of 30 K. This was already sufficiently high to

suggest to the superconductivity community that it might be difficult to explain using the usual form of the BCS theory, and a large number of related discoveries followed quickly. In the following year Wu et al. (Wu et al., 1987) found that the closely related material $YBa_2Cu_3O_{7-\delta}$ now known as YBCO, has a T_c of about 93 K when $\delta \sim 0.10$, well above the boiling point of liquid nitrogen (78 K). A few of the best known cuprate superconductors are listed in Table 3.1 Many other closely related compounds with similar transition temperatures are now known: the compound $HgBa_2Ca_2Cu_3O_{8+\delta}$, for instance, has a T_c as high as 150 K under pressure (Chu et al., 1993). There are also superconducting metallic compounds of other types. For instance, $BaBi_{0.25}Pb_{0.75}O_3$ is a perovskite containing no copper, with a T_c of 13 K. Some oxides with spinel structures and some metal chalcogenides are also superconducting. However, all known superconductors with T_c>50 K are perovskite cuprate superconductors.

Table 3.1: The best known cuprate superconductors, showing the stacking of planes in the *c* direction. (Waldram, 1996)

$La_{2-x}Sr_xCuO_4$	$YBa_2Cu_3O_{6+x}$	$Bi_2Sr_2CaCu_2O_{8+x}$	$Tl_2Ba_2Ca_2Cu_3O_{10+x}$
La/Sr cuprate	YBCO 123	Bi 2212	Tl 2223
$T_c = 38$ K	$T_c = 93$ K	$T_c = 94$ K	$T_c = 125$ K
			CuO_2
	CuO_2	CuO_2	Ca
CuO_2	Y	Ca	CuO_2
	CuO_2	CuO_2	Ca
			CuO_2
(La/Sr)O	BaO	SrO	BaO
(La/Sr)O	CuO_x	$BiO_{1+x/2}$	$TlO_{1+x/2}$
	BaO	$BiO_{1+x/2}$	$TlO_{1+x/2}$
		SrO	BaO

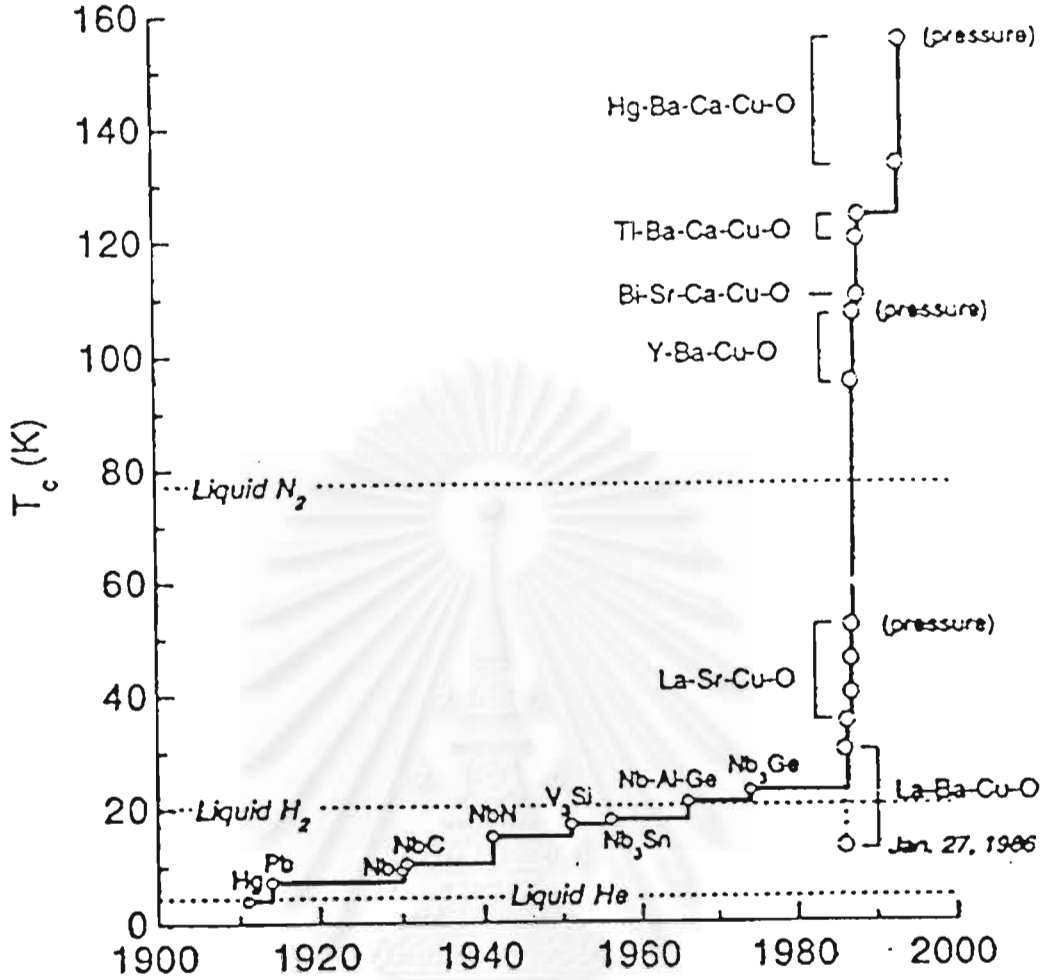

Figure 3.1: Maximum superconducting critical temperature T_c versus date. (Maple, 1998)

Apart from their high T_c values, the cuprate superconductors have a number of features in common, which make them very unlike typical low T_c metal superconductors. First, they are layer compounds. They are typically tetragonal, or orthorhombic and close to tetragonal, and contain Cu-O planes with the formula CuO_2 lying normal to the *c* direction. These planes contain mobile charge carriers and are thought to be the seat of the superconductivity.

The carriers are usually sharply localized in the planes, and this makes contact between the planes relatively weak. For this reason the cuprates often have extremely anisotropic properties, in both the normal and the superconducting states, with poor conduction in the c direction. Secondly, the carrier density is relatively low comparable with what is found in semi-metals such as bismuth. This means that the carriers are less heavily screened than they are in ordinary metals and makes the Coulomb repulsion between them more important. It also increases the penetration depth λ, which is typically 0.2 μm for current flow within the $a-b$ plane. Thirdly, they all have extremely short coherence lengths ξ, typically 2 nm within the CuO_2 planes and as little as 0.3 nm in the c direction. This has many important consequences. It makes thermal fluctuations much larger. It also makes defects such as impurity concentrations, grain boundaries and surface rearrangements much more important. Finally, all cuprates are very sensitive to carrier doping, and are only superconducting for a particular range of doping levels, which often requires non-stoichiometric compositions, as we have seen. This is perhaps the chief reason why they were not discovered earlier.

3.3 Structure of Cuprate Superconductors

The ideal perovskite structure ABX_3 is shown in Fig. 3.2(a). This structure is cubic. The anion X (typically oxygen) and the cation A (typically Sr or Ba in the case of cuprate superconductors) have relatively large ionic radii and are in contact, they determine the size of the structure. The B cation (Cu for the

cuprates) is smaller and occupies some of the interstices of the A–X network. It is coordinated by six anions, forming an octahedron.

However, as we noted is Section 3.2, the cuprate superconductors are complex tetragonal or almost tetragonal materials and do not have the simple perovskite structure just described. (Indeed, a $BaCuO_3$ perovskite is not possible although it would have had compatible ionic radii, it would not have been electrically neutral for any normal valences of Cu.) However, several important features of the ideal perovskite structure are present in the cuprates (Table 3.1 and Fig. 3.2(b)). First, and most important, we have CuO_2 planes in the $a-b$ plane, with a simple square lattice whose cell side is about 0.38 nm. This is a little less than would be allowed by consideration of ionic radii, which is explained, as we shall see later, by the fact that the planes have a partly covalent or metallic character. Secondly, the CuO_2 planes in the $a-b$ plane are often adjacent to purely ionic interleaving AX planes, so that the O atoms of the interleaving plane coordinate the Cu atoms of the CuO_2 plane as in the perovskite structure. Thirdly, the picture of a rectangular framework of large anions and cations in contact, with smaller cations in the interstices, survives.

The situation is best understood by treating both the conducting CuO_2 layers and the interleaved ionic BaO (or SrO) layers as capable of expansion in the c direction. In some cuprates the copper layers are isolated as in the perovskites, but in others we may have two or three (or more) layers stacked

directly above each other, with small cations in the interstices between them, as shown in Table 3.1. The interleaved ionic layers, too, are often expanded. In lanthanum cuprates, for instance, we have double interleaved layer (LaO)(LaO): successive individual layers are of course offset in the $x-y$ plane so that the cations of one layer lie above the anions of the next. Following the pattern apparent in the table, we are not surprised to find that the Tl compounds form a general series of compounds with the formulae $[(CuO_2)_n Ca_{n-1}][(TlO)_m(BaO)_2]$, in which T_c rises with n. The Bi compounds form a similar series in which TlO is replaced by BiO. Other compounds are formed by appropriate substitution within this pattern, for instance, the compound $HgBa_2Ca_2Cu_3O_{8+\delta}$ with very high T_c (referred to in Section 3.2) has the $n=3$, $m=1$ structure $[(CuO_2)_3Ca_2][Hg(BaO)_2]$, with the Hg taking the place of a TlO layer. The complexity does not end here. In some cuprates, such as the bismuth compounds, the layer structure is very variable and may show complex superstructure in the z direction.

The structures must of course be electrically neutral. The state of the CuO_2 layers depends on how the compound is doped. For the moment we consider the parent compound from which the superconducting compound may be obtained by doping. In the parent compound we shall treat the CuO_2 planes as being made up of Cu^{2+} and O^{2-} ions, so the planes have a negative charge and the ionic interleaved planes a positive charge. For instance, in

lanthanum cuprates we note that the double interleaved layer has a net charge of +2 units per unit cell, which compensates for the negative charge on the single copper layer.

When the systems are doped to make the CuO_2 layers superconducting, the dopants are normally in the interleaved layers, and not in the CuO_2 layers themselves. The dopants are either substitute cations with a different valency, such as Sr^{2+} for La^{3+} or Bi^{3+}, or oxygen vacancies, or extra oxygen inserted into vacant sites by a suitable heat treatment, or a mixture of these. In most cases as we have noted the interleaved layers are ionic with no free carriers, and the doping charge is therefore taken up as a change in the effective Cu valency in the CuO_2 layers, with a corresponding change in the carrier density available in those layers. An important exception to this picture arises in YBCO and related compounds, where, confusingly, the expanded interleaved layer also contains Cu, having the structure $(BaO)(CuO_x)(BaO)$, and the doping is altered by changing the O concentration in the CuO_x layer. In this layer the structure stable at low temperatures and high oxygen contents has CuO chains running in the *b* direction, with O vacancies on the chains (Fig. 3.1(b)). The CuO chains, like the CuO_2 planes, contain free carriers and contribute to the normal conductivity; there is also some evidence that they contribute to the supercurrent.

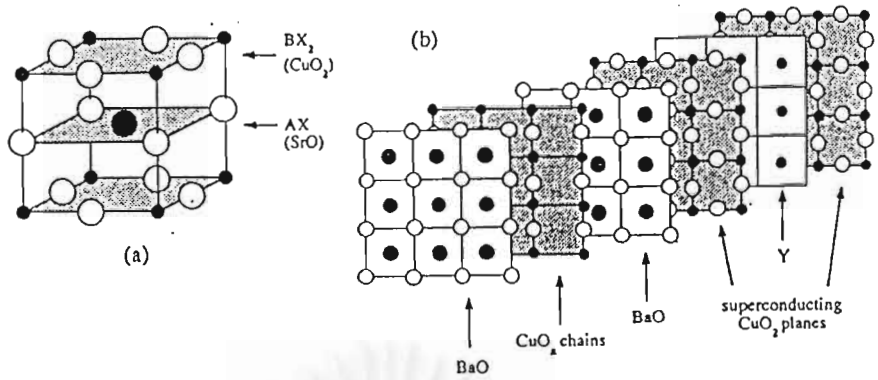

Figure 3.2: (a) The perovskite structure ABX_3, showing the BX_2 planes which correspond to the CuO_2 planes of the cuprate superconductors, and the AX planes, which correspond to the SrO or BaO planes. (b) Stacking of planes in YBCO: the planes are really stacked vertically, but have been displaced to make their structure visible. Note the Cu-O chains in the interleaving plane. (Waldram, 1996)

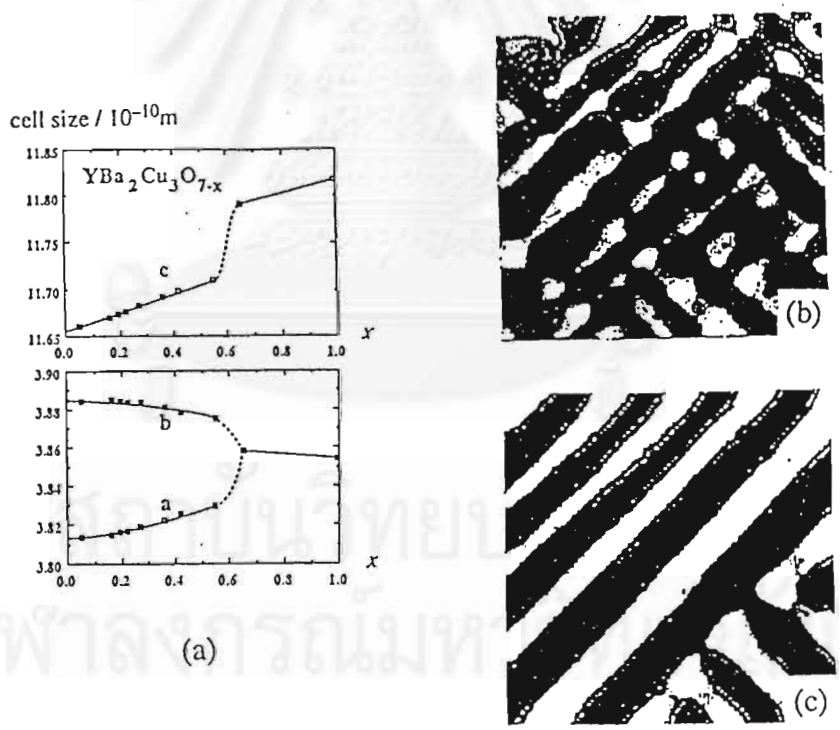

Figure 3.3: (a) Orthorhombic-tetragonal transition in YBCO as a function of oxygen concentration. (b) Simulation of the tweed pattern of microtwins generated by the transition in YBCO at low temperatures. The shading indicates the local cell distortion. (c) Corresponding simulation of the stripe pattern which appears on annealing. (Waldram, 1996)

3.4 Tetragonal–Orthorhombic Transition and Twinning

The chains in the YBCO 123 structure make the lattice orthorhombic, with b very slightly greater than a, but at high temperatures and low O concentration the O positions in the planes containing the chains become randomized and the system becomes tetragonal with $a = b$ (Fig. 3.3(a)). Large concentrations of vacancies and antisite disorder in the doping layers are common in cuprates, and other systems besides the 123 structure become slightly orthorhombic at low temperatures.

Since the crystals are usually grown at high temperatures where the structures are tetragonal, internal stresses make the orthorhombic material microtwinned at low temperatures unless special precautions are taken, with twin boundaries lying in the $\{110\}$ directions and the a and b directions exchanged in adjacent crystallites. When the twins are first formed in YBCO, twin boundaries usually appear on both sets of $\{110\}$ directions at a spacing of about 10 nm, the two sets intersecting at right angles, producing a characteristic tweed pattern of microcrystallites which form crossing rectangles (Fig. 3.3(b)). The twin boundary intersections involve extra elastic energy, and successive microcrystallites are slightly rotated in opposite directions. On annealing, the system may develop a stripe pattern in which one set of domain walls is suppressed and the microcrystallites form long parallel stripes, the direction now alternating on a scale considerably longer

than the stripe spacing (Fig. 3.3(c)). The tweed pattern may, however, be stabilized in O-depleted or Co-doped samples.

It is possible but difficult to prepare twin-free crystals. Note that microtwinning is almost invariably present in what may seem to be good single crystals of YBCO and other 123 structures. Its effects on measured physical properties have not, to date, been systematically investigated, may be substantial and are not always properly appreciated.

3.5 The Van Hove Scenario

The idea of the Van Hove scenario (Tsuei et al., 1990, 1992), (Newns, et al., 1992) in its essence is that many of the special properties of the cuprate superconductors are attributable to the presence close to the Fermi level of saddle points in the band-structure energy surface. These are found to have strong implications in two-dimensional (2D) or nearly 2D electron systems such as the cuprate materials are known to be. Associated with the saddle points (SP's), that are flat regions of the energy dispersion, is the logarithmic (in two dimensions) singularity in the density of states (Tsuei et al., 1990, 1992), (Newns, et al., 1992), know as the Van Hove singularity (VHS).

Three basic effects (at least) of the SP's on electronic properties have been detailed. First, the superconducting transition temperature is enhanced by having a DOS peak near the Fermi energy (Tsuei et al., 1990, 1992), (Newns, et al., 1992), (Friedel, 1989), (Labbe′ and Bok, 1987), (Markiewicz, 1990, 1992), so that as the Fermi energy (experimentally, this can be controlled by

doping) is swept though the VHS, the transition temperature goes through a maximum at the point where the VHS and the Fermi energy coincide.

Secondly, there is a qualitative enhancement in the scattering between quasiparticles (Tsuei et al., 1990, 1992), (Newns, et al., 1992, 1994), (Pattnaik et al., 1992). In a conventional metal, direct quasiparticle-quasiparticle scattering is almost completely suppressed, because it is nearly impossible to find significant phase space for a pair of quasiparticles to scatter into, given the thinness of the shell of thermally excited quasiparticles around the Fermi surface, relative to the Fermi energy E_F. But analysis shows (Tsuei et al., 1990, 1992), (Newns, et al., 1992, 1994), (Pattnaik et al., 1992) that when the VHS and E_F coincide, or the relative energy (Newns, et al., 1994), (Pattnaik et al., 1992) of the VHS and E_F are within temperature T, the phase space for scattering is much less restricted, leading to the "marginal-Fermi-liquid" (MFL) property (Tsuei et al., 1990, 1992), (Newns, et al., 1992, 1994), (Pattnaik et al., 1992) that lifetime broadening for the quasiparticles is of the order of their energy measured from E_F.

The third effect (Tsuei et al., 1990, 1992), (Newns, et al., 1992) of having the VHS close to E_F is that the realistic Fermi surface (see Fig. 3.4) does not have a significant flat portion (note the area inside the surface differs from that outside by doping). This absence of flat portions inhibits "nesting" scattering which, in the metallic phase, enhances antiferromagnetic spin-

density-wave (SDW) or charge-density-wave (CDW) instabilities. These are the strongest competing instabilities for superconductivity.

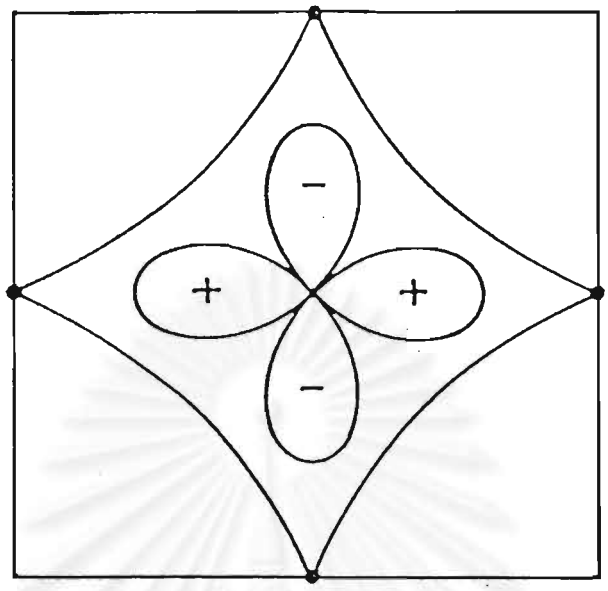

Figure 3.4: Idealized Fermi surface in Van Hove scenario, showing saddle points (dark circles) and lobes of $d_{x^2-y^2}$ order parameter. (Newns, Tsuei, and Pattnaik, 1995)

Experimentally, the saddle points near E_F are indeed seen directly in angle-resolved photoemission spectroscopy experiments (Abrikosov et al., 1993), (Gofron et al., 1994), (Dessau et al., 1993), (King et al., 1993) on maximal-T_c materials. Analysis of the specific-heat-jump data (Tsuei et al., 1990, 1992), (Newns, et al., 1992) supports the presence of the VHS in the DOS. The MFL behavior seems to underlie transport anomalies such as the linear resistivity (Tsuei et al., 1990, 1992), (Newns, et al., 1992, 1994), (Pattnaik et al., 1992) and T-independent thermopower (Pattnaik et al., 1992), (Newns, et al., 1994), which also are associated with the vicinity of maximal T_c. And the correlation length for the SDW instability (expected to dominate

CDW for repulsive interactions) is short, of order one lattice spacing, near maximal T_c. This experimental picture is entirely consistent with the Van Hove scenario.

3.6 Van Hove Singularity in the Density of States

In the cuprate, it is well known that the CuO_2 plane contains three orbitals, Cu $d_{x^2-y^2}$ and $O(p_x, p_y)$ orbitals with a lope pointing towards to the Cu. This is the standard three-band model. The nature of the band structure of two-dimensional lattice is the energy surface has the singularity. We will investigate how a saddle point can cause the divergence in the electron density of states, we begin with the expression of the density of states

$$N(E) = \frac{1}{(2\pi)^3}\int d\mathbf{k}\,\delta(E - E(\mathbf{k})). \tag{3.1}$$

On the other hand the density of states in the energy surface between E and $E + dE$ is

$$N(E)dE = \int \frac{dS}{(2\pi)^3}\delta k(\mathbf{k}) \tag{3.2}$$

where $\delta k(\mathbf{k})$ is the perpendicular distance between the energy surfaces $S(E)$ and $S(E + dE)$ at the point $\mathbf{k}$. To find an explicit expression for $\delta k(\mathbf{k})$ we note that, the k-gradient of $E(\mathbf{k})$, $\nabla E(\mathbf{k})$, is a vector normal to that surface whose magnitude is equal to the rate of change of $E(\mathbf{k})$ in the normal direction; i.e.,

$$E + dE = E + |\nabla E(\mathbf{k})|\delta k(\mathbf{k}), \tag{3.3}$$

and hence

$$\delta k(\mathbf{k}) = \frac{dE}{|\nabla E(\mathbf{k})|}. \tag{3.4}$$

Thus we obtain the electron density of states in an alternative form

$$N(E) = \int \frac{dS}{(2\pi)^3} \frac{1}{|\nabla E(\mathbf{k})|}. \tag{3.5}$$

When $\nabla E(\mathbf{k})$ vanishes, the density of states diverges. This is known as Van Hove Singularities.

Next, we consider an orthorhombic lattice as a simplified model of the high-T_c Cu-O oxide. Its band structure is assumed to be modeled by a tight-binding band (Wang et al., 1987)

$$E(\mathbf{k}) = -2t\cos k_x - 2t_b \cos k_y + 4t_2 \cos k_x \cos k_y - 2t' \cos k_z \tag{3.6}$$

Here t, t_b, and t' are the hopping integrals between nearest-neighbor Cu sites, along the a, b, and c axes, respectively and t_2 is the hopping matrix element of next-nearest-neighbor ones in the same Cu-O planes. We introduce a set of dimensionless variable: $r_1 = t_b / t$, $r_2 = 2t_2 / t$, and $r' = t'/t$. For the system under consideration, the anisotropic parameter r' is assumed to be much smaller than unity $(r' << 1)$, indicating that the interplanar hopping is very small compare with the interplanar one. r_1 stands for the anisotropy within the Cu-O planes. Its introduction stems from the fact that the high-T_c superconducting samples are often in the orthorhombic phase in which there is a slight difference in length between the lattice parameters along the a and b axis. So

we can assume that r_1 is very close to, but slightly smaller than, unity. Since t_2 is always much smaller than t, it is reasonable to assume that $r_2 < r_1$.

In this section we first neglect the interplanar hopping (letting $t' = 0$) and study the case of a 2D rectangular lattice. The corresponding electron density of states is given by the expression

$$N(E) = \frac{1}{\pi^2} \int_0^{\pi} dk_x \int_0^{\pi} dk_y \, \delta(E - 2tW(k_x, k_y)), \tag{3.7}$$

where $W(k_x, k_y) = -\cos k_x - r_1 \cos k_y + r_2 \cos k_x \cos k_y$. We make a change of variables into v and w: $v = \cos k_y$ and $w = W(k_x, k_y)$. The δ function can be used to integrate over w, so the remaining integral over v is

$$N(E) = \frac{1}{2t\pi^2} \int_{v_1}^{v_2} \frac{dv}{\sqrt{[1 - v^2][(1 - r_2 v)^2 - (\varepsilon + r_1 v)^2]}} \tag{3.8}$$

with $\varepsilon = E/(2t)$. Here the upper and lower integration limits of the integral are

$$\begin{aligned} v_2 &= \min[1, (1-\varepsilon)/(r_1 + r_2)] \\ v_1 &= \max[-1, -(1+\varepsilon)/(r_1 - r_2)]. \end{aligned} \tag{3.9}$$

It then follows that there may be three kinds of integration limits in Eq.(3.8). They are $v_1 = -1$, $v_2 = (1-\varepsilon)/(r_1 + r_2)$ for $1 + r_1 + r_2 \geq \varepsilon \geq 1 - r_1 - r_2$; $v_1 = -1$, $v_2 = 1$ for $1 - r_1 - r_2 \geq \varepsilon \geq -1 + r_1 - r_2$; and $v_2 = 1$, $v_1 = -(1+\varepsilon)/(r_1 - r_2)$ for $-1 + r_1 - r_2 \geq \varepsilon \geq -1 - r_1 + r_2$, respectively. Making use of the integral formula (3.147.5) of Gradshteyn and Ryzhik (Gradshteyn and Ryzhik, 1965), we obtain for $N(E)$ the analytical expressions

$$N(E) = \frac{1}{2t\pi^2\sqrt{r_1 + r_2\varepsilon}} K\left[\frac{\sqrt{(1+r_1)^2 - (\varepsilon - r_2)^2}}{\sqrt{4(r_1 + r_2\varepsilon)}}\right] \tag{3.10}$$

for $1 + r_1 + r_2 \geq \varepsilon \geq 1 - r_1 - r_2$ or $-1 + r_1 - r_2 \geq \varepsilon > -1 - r_1 + r_2$, and

$$N(E) = \frac{1}{t\pi^2\sqrt{(1+r_1)^2 - (\varepsilon - r_2)^2}} K\left[\frac{\sqrt{4(r_1 + r_2\varepsilon)}}{\sqrt{(1+r_1)^2 - (\varepsilon - r_2)^2}}\right] \tag{3.11}$$

for $1 - r_1 - r_2 \geq \varepsilon \geq -1 + r_1 - r_2$, where $K(x) = F(\pi/2, x)$ is the complete elliptic integral of the first kind (Gradshteyn and Ryzhik, 1965). According to Eqs. (3.10) and (3.11), $N(E)$ is shown as a function of ε in Fig. 3.4, in which the $N(E)$ exhibits two singular peaks at $\varepsilon_+ = 1 - r_1 - r_2$ and $\varepsilon_- = -1 + r_1 - r_2$. Taking into account the asymptotic formula $K(x) = \ln[4(1 - x^2)^{-1/2}]$ with $x \approx 1$, we obtain for $N(E)$, near the singularities $\varepsilon_\pm$, the approximate expression

$$N(E) = \frac{1}{2t\pi^2\sqrt{(1 \mp r_2)(r_1 \pm r_2)}} \ln\left[\frac{8\sqrt{(1 \mp r_2)(r_1 \pm r_2)}}{\sqrt{2(\varepsilon - \varepsilon_\pm)(1 - r_1)}}\right]. \tag{3.12}$$

It can be seen from Fig. 3.4 that the appearance of two singularities in $N(E)$ originated from the orthorhombicity of the structure $(r_1 \neq 1)$, the distance between them being equal to $\varepsilon_+ - \varepsilon_- = 2(1 - r_1)$. As the rectangular to square lattice transition occurs (i.e., $r_1 = 1$), double Van Hove singularities at ε_+ and ε_- merge into a single one (Hirsch and Scalapino, 1986) at $\varepsilon_+ = \varepsilon_- = -r_2$, which is just the most used model (Wang et al., 1987), (Tsuei et al., 1990). So, we can conclude that the orthorhombicity of the structure leads to two sharp

peaks in $N(E)$, but it does not change the logarithmic Van Hove singularity so long as the interplanar hopping is weak enough to be negligible.

We consider a 2D square lattice of $r_1 = 1$, for which there is only a Van Hove singularity in $N(E)$ at $\varepsilon_{\pm} = -r_2$. According to Eq.(3.10) or Eq.(3.11), the density of states near this singularity has the following form:

$$N(E) = N_0\left[\ln\left|\frac{E_F}{E - E_s}\right| + C\right] \tag{3.13}$$

with $N_0^{-1} = 2t\pi^2\sqrt{1-r_2^2}$, $C = \ln|16t\sqrt{1-r_2^2}/E_F|$, and $E_s = -2t\,r_2$. These results are derived by Xing, Liu, and Gong (Xing, Liu, and Gong, 1991).

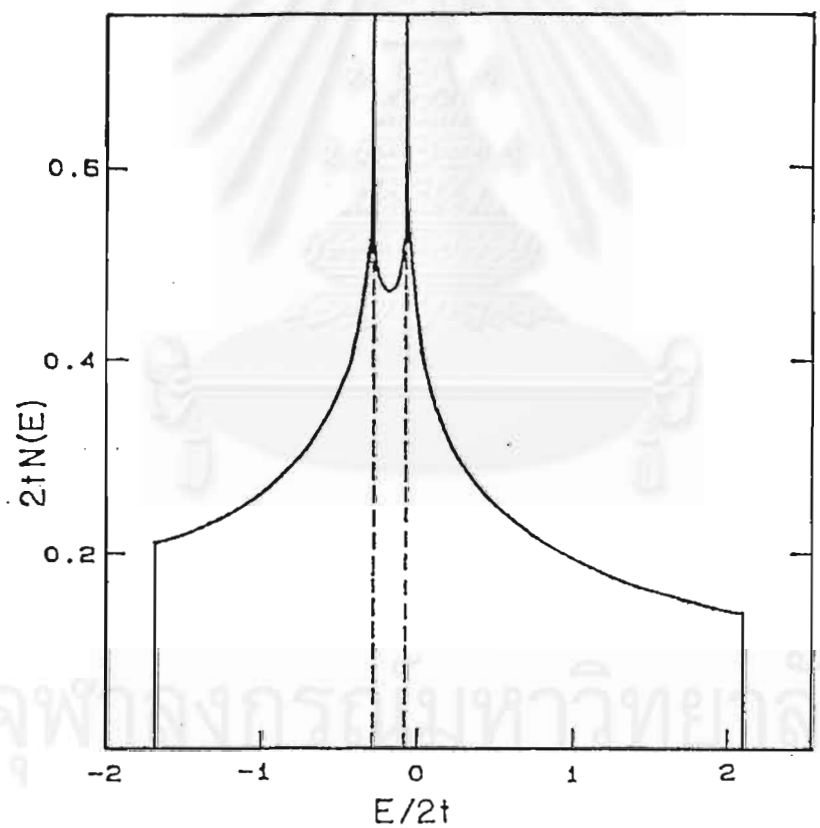

Figure 3.5: Density of states, $N(E)$, for $r_1 = 0.9$ and $r_2 = 0.2$. The singularities occur for $\varepsilon_+ = 1 - r_1 - r_2 = -0.1$ and $\varepsilon_- = -1 + r_1 - r_2 = -0.3$. (Xing, Liu, and Gong, 1991)

Chapter 4

Specific Heat Jump at T_c of High-T_c Superconductors

4.1 Introduction

It is well known that the Van Hove scenario can explain many physical properties of high-T_c superconductor such as the high value of T_c, anomalous isotope effect, etc (Labbe′ and Bok, 1987). Labbe′ and Bok used a two-dimensional band structure calculation for alkaline-earth-substituted La_2CuO_4 in the tetragonal phase. Within the framework of the BCS phonon-mediated pairing, Tsuei et al. (Tsuei et al., 1990) showed that a logarithmic (2D) Van Hove Singularity (VHS) in the density of states can provide a basis for understanding the anomalous isotope effects in the Y-Ba-Cu-O and the Bi-Sr-Ca-Cu-O systems. In the experimental work of Wühl et al. (Wühl et al., 1991) and Däumling (Däumling, 1991), they measured $\Delta C/T_c$ for high-quality oxygen-deficient $YBa_2Cu_3O_{7-y}$ polycrystalline samples ($0 < y < 0.43$). The thermodynamic properties such as the specific-heat discontinuity at the transition temperature (T_c), $\Delta C/T_c$, and the zero-temperature critical field, $H_c(0)$, of the oxygen-deficient YBa_2CuO_{7-y} were analyzed, by Tsuei et al. (Tsuei et al., 1992), to show that the density of states at the Fermi level is

peaked at y=0 and consistent with the Fermi level lying close to a two-dimensional Van Hove Singularity.

However, while many aspects of the high-T_c superconductors (transition temperature (Labbe′ and Bok, 1987), (Friedel, 1989), (Tsuei et al., 1990, 1992), (Markiewicz, 1990, 1992), (Newns et al., 1992) isotope shift (Tsuei et al., 1990, 1992), specific-heat jump (Tsuei et al., 1990, 1992)) have been worked out on the basis of s-wave pairing, experiments (Takigawa et al., 1991), (Takigawa and Mitzi, 1994), (Sonier et al., 1993), (Tsuei et al., 1994), (Wollman et al., 1994) seem to increasingly favor d-wave pairing, in the particular $d_{x^2-y^2}$, pairing. For example, measurements (Takigawa et al., 1991), (Takigawa and Mitzi, 1994) of the NMR nuclear spin-lattice relaxation rate $1/T_1$ below T_c, the low-temperature magnetic penetration depth (Sonier et al., 1993), and measurements of the phase of the order parameter (Tsuei et al., 1994), (Wollman et al., 1994) seem to pose insurmountable problems for an s-wave interpretation. Recently Newns et al. (Newns et al., 1995) used the assumption that the pairing is $d_{x^2-y^2}$ symmetry in an investigation of transition temperature, gap, and specific-heat jump at the BCS level of approximation. They found that the effect of the d-wave pairing and the Van Hove Singularity on these properties is similar to, and at least as strong as, the effect in s-wave. The d-wave version of the Van Hove scenario was therefore found to be fully viable. Dorbolo et al. (Dorbolo et al., 1996) studied the

influence of a logarithmic VHS on the electronic specific heat C_e of a 2D superconductor. The theoretical results were obtained for an isotropic s-wave gap parameter and an anisotropic $d_{x^2-y^2}$-wave gap parameter. They found that the magnitude of the specific heat jump at T_c observed in high-T_c superconductors can be reproduced by considering both gap parameter symmetries. They also found that the very low temperature behavior of C_e as observed in a single crystal of $YBa_2Cu_3O_{7-\delta}$ is only consistent only with a gap parameter of the $d_{x^2-y^2}$-wave type.

In this chapter, in order to understand the thermodynamic properties of the high-temperature superconductivity within the framework of BCS theory, we will study the specific heat jump at the transition temperature T_c. We consider the effects of the density of states (DOS) (both the constant DOS and the VHS DOS) as well as the types of pairing (s and d) on the specific heat jump.

The specific heat C of a material is defined as the change in internal energy U brought about by a change in temperature

$$C = \left(\frac{dU}{dT}\right)_v . \tag{4.1}$$

We will not make a distinction between the specific heat at constant volume and the specific heat at constant pressure because for solids these two properties are virtually indistinguishable. Ordinarily, the specific heat is

measured by determining the heat input dQ needed to raise the temperature of the material by an amount dT,

$$dQ = CdT \tag{4.2}$$

The conduction electron contribution C_e to the specific heat is given by the derivative dE_T/dT when E_T is the total electron energy.

4.2 Temperature Dependence of the Order Parameter and Specific Heat Jump at T_c

Within the BCS framework , the gap equation is given by the equation

$$\Delta_{\mathbf{k}} = \sum_{\mathbf{k}'} \frac{V_{\mathbf{kk}'}\Delta_{\mathbf{k}'} \tanh(\frac{E_{\mathbf{k}'}}{2T})}{2E_{\mathbf{k}'}} \tag{4.3}$$

here $E_{\mathbf{k}}^2 = (\varepsilon_{\mathbf{k}} - E_F)^2 + \Delta_{\mathbf{k}}^2$, $\varepsilon_{\mathbf{k}}$ is the quasiparticle energy, E_F is the Fermi energy , $\Delta_{\mathbf{k}}$ is the order parameter , $V_{\mathbf{kk}'}$ is the positive phonon mediated interaction which is finite within the energy range of $\hbar\omega_D$ around E_F and ω_D is the Debye frequency. For the sake of simplicity we assume that

$$V_{\mathbf{kk}'} = V\, g(\phi)g(\phi') \text{ , if } E_F - \hbar\omega_D \le \varepsilon_{\mathbf{k}}, \varepsilon_{\mathbf{k}'} \le E_F + \hbar\omega_D \tag{4.4}$$

and $g(\phi) = 1$ or $\cos 2\phi$ depending on whether the superconductor is an s- or d-wave one, here ϕ is the angle between the momentum $\mathbf{k}$ of the pair electrons and the a-axis of a CuO_2 plane, i.e. $\phi = \tan^{-1}(k_y/k_x)$ and V represents the constant electron-phonon interaction strength.

For the form of the scattering matrix element given by Eq.(4.4), the solution of the gap equation has the structure

$$\Delta_k = \Delta(T)g(\phi) \tag{4.5}$$

where $\Delta(T)$ is the temperature-dependent energy gap function. Upon substituting Eqs.(4.4) and (4.5) in Eq.(4.3) , one obtains the equation

$$\frac{1}{V} = \int_0^{2\pi} \frac{d\phi}{2\pi} g^2(\phi) \int_{-\omega_D}^{\omega_D} \frac{d\varepsilon}{2E} N(\varepsilon) \tanh(\frac{E}{2T}) \tag{4.6}$$

here $N(\varepsilon)$ is the electronic density of states per spin and $E = \sqrt{\varepsilon^2 + \Delta^2(T)g^2(\phi)}$.

By differentiating Eq.(4.6) with respect to T, the result is

$$0 = \int_0^{2\pi} \frac{d\phi}{2\pi} g^2(\phi) \int_{-\omega_D}^{\omega_D} \frac{d\varepsilon}{2} N(\varepsilon) \frac{\partial}{\partial T}\left[\frac{1}{E}\tanh(E/2T)\right] \tag{4.7}$$

We now consider the term

$$\begin{aligned}
&\frac{\partial}{\partial T}\left[\frac{1}{E}\tanh(E/2T)\right] \\
&= \left[-\frac{1}{E^2}\tanh(E/2T) + \frac{1}{2ET}\operatorname{sech}^2(E/2T)\right]\frac{\partial E}{\partial T} - \frac{1}{2T^2}\operatorname{sech}^2(E/2T) \\
&= \frac{1}{2}\left\{\left[-\frac{1}{E^3}\tanh(E/2T) + \frac{1}{2E^2T}\operatorname{sech}^2(E/2T)\right]g^2(\phi)\frac{d\Delta^2(T)}{dT} - \frac{1}{T^2}\operatorname{sech}^2(E/2T)\right\}.
\end{aligned} \tag{4.8}$$

Substituting Eq.(4.8) in Eq.(4.7), and manipulating them we obtain the temperature gradient of $\Delta^2(T)$ as follows

$$\frac{d\Delta^2(T)}{dT} = \frac{\frac{1}{T^2}\int_0^{2\pi}\frac{d\phi}{2\pi}g^2(\phi)\int_{-\omega_D}^{\omega_D}\frac{d\varepsilon}{2}N(\varepsilon)\operatorname{sech}^2(E/2T)}{\int_0^{2\pi}\frac{d\phi}{2\pi}g^4(\phi)\int_{-\omega_D}^{\omega_D}\frac{d\varepsilon}{2}N(\varepsilon)\left[\frac{\operatorname{sech}^2(E/2T)}{2TE^2} - \frac{\tanh(E/2T)}{E^3}\right]} \tag{4.9}$$

Since E reduces to ε when $T = T_c$, by letting the variable $x = \varepsilon / 2T_c$ and using the notation $\langle g^n(\phi) \rangle = \int_0^{2\pi} \frac{d\phi}{2\pi} g^n(\phi)$, Eq.(4.9) can be written as

$$\frac{d\Delta^2(T)}{dT}\Big|_{T=T_c} = \frac{8T_c \langle g^2(\phi) \rangle \int_0^{\omega_D/2T_c} dx\, N(2T_c x)\, \mathrm{sech}^2(x)}{\langle g^4(\phi) \rangle \int_0^{\omega_D/2T_c} dx\, N(2T_c x) \left[\frac{\mathrm{sech}^2(x)}{x^2} - \frac{\tanh(x)}{x^3} \right]}. \tag{4.10}$$

The jump in the specific heat T_c within the framework of the BCS formalism is calculated from the usual expressions for specific heat of the normal and superconducting phases given by

$$C_N = 2 \sum_k \varepsilon_k \frac{\partial f(\varepsilon_k)}{\partial T} \tag{4.11}$$

$$C_S = 2 \sum_k E_k \frac{\partial f(E_k)}{\partial T}. \tag{4.12}$$

Here the indices N and S denote the normal and superconducting states, respectively. $f(\varepsilon_k)$ is the usual Fermi distribution function for electron with the wave vector $\mathbf{k}$. The factor 2 arises for the sum over spins of the Cooper pair. The expression for the Fermi distribution function has the form

$$f(\varepsilon_k) = \frac{1}{1 + e^{\varepsilon_k / T}} \tag{4.13}$$

The temperature derivative of Eq.(4.13) is

$$\frac{\partial f(\varepsilon_k)}{\partial T} = \frac{\varepsilon_k}{4T^2} \mathrm{sech}^2(\varepsilon_k / 2T) \tag{4.14}$$

By inserting Eq.(4.14) in Eq.(4.11) and transform the sum to an integral form, we get

$$C_N(T) = \frac{1}{2T^2}\int_{-\infty}^{\infty} d\varepsilon\, N(\varepsilon)\varepsilon^2 \mathrm{sech}^2(\varepsilon/2T) \tag{4.15}$$

Similarly for the superconducting phase

$$C_S(T) = \int_0^{2\pi}\frac{d\phi}{2\pi}\int_0^{\omega_D} d\varepsilon\, N(\varepsilon)\left\{\frac{E^2}{T^2}-\frac{1}{2T}g^2(\phi)\frac{d\Delta^2(T)}{dT}\right\}\mathrm{sech}^2(E/2T) \tag{4.16}$$

At $T = T_c$ we let $x = \varepsilon/2T_c$ then Eqs.(4.15) and (4.16) become

$$C_N(T_c) = 8T_c\int_0^{\infty} dx\, N(2T_c x)\, x^2 \mathrm{sech}^2(x) \tag{4.17}$$

and

$$\begin{aligned} C_S(T_c) = & -\left(\frac{d\Delta^2(T)}{dT}\Big|_{T=T_c}\right)\left\langle g^2(\phi)\right\rangle\int_0^{\omega_D/2T_c} dx\, N(2T_c x)\,\mathrm{sech}^2(x) \\ & + 8T_c\int_0^{\omega_D/2T_c} dx\, N(2T_c x)\, x^2 \mathrm{sech}^2(x) \end{aligned} \tag{4.18}$$

Inserting Eq.(4.10) in Eq.(4.18), we get

$$C_S(T_c) = \frac{-8T_c\left[\left\langle g^2(\phi)\right\rangle\int_0^{\omega_D/2T_c} dx\, N(2T_c x)\,\mathrm{sech}^2(x)\right]^2}{\left\langle g^4(\phi)\right\rangle\int_0^{\omega_D/2T_c} dx\, N(2T_c x)\left[\frac{\mathrm{sech}^2(x)}{x^2}-\frac{\tanh(x)}{x^3}\right] + 8T_c\int_0^{\omega_D/2T_c} dx\, N(2T_c x)\, x^2 \mathrm{sech}^2(x)} \tag{4.19}$$

We denote the difference of specific heat at a transition temperature between the superconducting and normal phases by $\Delta C(T_c)$, i.e.

$$\Delta C(T_c) = C_S(T_c) - C_N(T_c). \tag{4.20}$$

Substituting Eqs.(4.19) and (4.17) in Eq.(4.20), we find that

$$\Delta C(T_c) = 8T_c\left\{\int_0^{\omega_D/2T_c} dx\, N(2T_c x)x^2 \mathrm{sech}^2(x) - \int_0^{\infty} dx\, N(2T_c x)x^2 \mathrm{sech}^2(x) - \frac{\left[\left\langle g^2(\phi)\right\rangle \int_0^{\omega_D/2T_c} dx\, N(2T_c x)\mathrm{sech}^2(x)\right]^2}{\left\langle g^4(\phi)\right\rangle \int_0^{\omega_D/2T_c} dx\, N(2T_c x)\left[\frac{\mathrm{sech}^2(x)}{x^2} - \frac{\tanh(x)}{x^3}\right]}\right\}. \tag{4.21}$$

We finally obtain the ratio between the jump in the specific heat at a transition from the normal to the superconducting states and the normal specific heat as

$$\frac{\Delta C(T_c)}{C_N(T_c)} = \frac{1}{\int_0^{\infty} dx N(2T_c x)x^2 \mathrm{sech}^2(x)}\left\{\int_0^{\omega_D/2T_c} dx N(2T_c x)x^2 \mathrm{sech}^2(x) - \frac{\left[\left\langle g^2(\phi)\right\rangle \int_0^{\omega_D/2T_c} dx N(2T_c x)\mathrm{sech}^2(x)\right]^2}{\left\langle g^4(\phi)\right\rangle \int_0^{\omega_D/2T_c} dx N(2T_c x)\left[\frac{\mathrm{sech}^2(x)}{x^2} - \frac{\tanh(x)}{x^3}\right]}\right\} - 1. \tag{4.22}$$

4.3 Effect of the Constant Density of States

We note that Eqs.(4.9) and (4.22) are exact analytical expressions for the temperature gradient of $\Delta^2(T)$ and the normalized specific heat jump

$\frac{\Delta C(T_c)}{C_N(T_c)}$. In the standard BCS treatment, $N(\varepsilon)$ is assumed to be constant, independent of energy, i.e. $N(\varepsilon)=N(0)$. The Eq.(4.22) becomes

$$\frac{\Delta C(T_c)}{C_N(T_c)} = \frac{\int_0^{\omega_D/2T_c} dx\, x^2 \mathrm{sech}^2(x)}{\int_0^{\infty} dx\, x^2 \mathrm{sech}^2(x)} - 1 - \frac{\left[\left\langle g^2(\phi)\right\rangle \int_0^{\omega_D/2T_c} dx\, \mathrm{sech}^2(x)\right]^2}{\left\langle g^4(\phi)\right\rangle \int_0^{\infty} dx\, x^2 \mathrm{sech}^2(x) \int_0^{\omega_D/2T_c} dx \left[\frac{\mathrm{sech}^2(x)}{x^2} - \frac{\tanh(x)}{x^3}\right]} \tag{4.23}$$

After some integration procedures, we get the formulas

$$\int_0^{\infty} dx\, x^2 \mathrm{sech}^2(x) = \frac{\pi^2}{12}, \tag{4.24}$$

$$\int_0^{\omega_D/2T_c} dx\, x^2 \mathrm{sech}^2(x) = \left(\frac{\omega_D}{2T_c}\right)^2 \left[1+\tanh\left(\frac{\omega_D}{2T_c}\right)\right] - \frac{\omega_D}{T_c} \ln\left[2\cosh\left(\frac{\omega_D}{2T_c}\right)\right] + \mathrm{Li}_2(-e^{-\omega_D/T_c}) + \frac{\pi^2}{12}, \tag{4.25}$$

$$\int_0^{\omega_D/2T_c} dx\, \mathrm{sech}^2(x) = \tanh(\omega_D/2T_c), \tag{4.26}$$

$$\int_0^{\omega_D/2T_c} dx \left[\frac{\mathrm{sech}^2(x)}{x^2} - \frac{\tanh(x)}{x^3}\right] = \frac{\tanh(\omega_D/2T_c)}{(\omega_D/2T_c)^2} - \frac{1}{(\omega_D/2T_c)} - \frac{16}{\pi^3}\sum_{n=0}^{\infty} \frac{1}{(2n+1)^3} \tan^{-1}\left(\frac{\omega_D/\pi T_c}{2n+1}\right), \tag{4.27}$$

here $\mathrm{Li}_2(x)=\sum_{k=1}^{\infty}\frac{x^k}{k^2}$ is the dilogarithmic function (Abramowitz and Stegun, 1972) and substituting these integral formulas in Eq.(4.23), we finally obtain the exact form of the ratio between the jump in the specific heat at a transition from the normal to the superconducting states and the normal specific heat in any pairing states, i.e., s-wave or d-wave as

$$\frac{\Delta C(T_c)}{C_N(T_c)} = \frac{12}{\pi^2}\left(\left(\frac{\omega_D}{2T_c}\right)^2\left[1+\tanh\left(\frac{\omega_D}{2T_c}\right)\right]-\frac{\omega_D}{T_c}\ln\left[2\cosh\left(\frac{\omega_D}{2T_c}\right)\right]+\mathrm{Li}_2(-e^{-\omega_D/T_c})+\frac{\pi^2}{12}\right)-1 - \frac{\left\langle g^2(\phi)\right\rangle^2\tanh^2(\omega_D/2T_c)}{\left\langle g^4(\phi)\right\rangle\left(\frac{\tanh(\omega_D/2T_c)}{(\omega_D/2T_c)^2}-\frac{1}{(\omega_D/2T_c)}-\frac{16}{\pi^3}\sum_{n=0}^{\infty}\frac{1}{(2n+1)^3}\tan^{-1}\left(\frac{\omega_D/\pi T_c}{2n+1}\right)\right)} \tag{4.28}$$

In the case of s-wave pairing state, $g(\phi)=1$, Eq.(4.28) reads

$$\frac{\Delta C(T_c)}{C_N(T_c)} = \frac{12}{\pi^2}\left\{\left(\frac{\omega_D}{2T_c}\right)^2\left[1+\tanh\left(\frac{\omega_D}{2T_c}\right)\right]-\left(\frac{\omega_D}{T_c}\right)\ln\left[2\cosh\left(\frac{\omega_D}{2T_c}\right)\right]+\mathrm{Li}_2(-e^{-\omega_D/T_c}) - \frac{\tanh^2(\omega_D/2T_c)}{\frac{\tanh(\omega_D/2T_c)}{(\omega_D/2T_c)^2}-\frac{1}{(\omega_D/2T_c)}-\frac{16}{\pi^3}\sum_{n=0}^{\infty}\frac{1}{(2n+1)^3}\tan^{-1}\left(\frac{\omega_D/\pi T_c}{2n+1}\right)}\right\}. \tag{4.29}$$

In the limit $\omega_D/T_c\to\infty$, Eq.(4.29) reduces to $\frac{\Delta C(T_c)}{C_N(T_c)}=\frac{12}{7\zeta(3)}=1.43$ which is identical to the standard classical BCS value shown in Fig. 4.1, here $\zeta(3)$ is the Riemann zeta function and $C_N(T_c)=\frac{2}{3}\pi^2N(0)T_c$.

Our exact result shows that $\frac{\Delta C(T_c)}{C_N(T_c)}$ is material dependent and depends only on the ratio ω_D/T_c. Our graphical computation of Eq.(4.29) shows that the curve of $\frac{\Delta C(T_c)}{C_N(T_c)}$ versus ω_D/T_c increases monotonically as ω_D/T_c increases and reaches its constant value of 1.43 when ω_D/T_c is greater than 7.

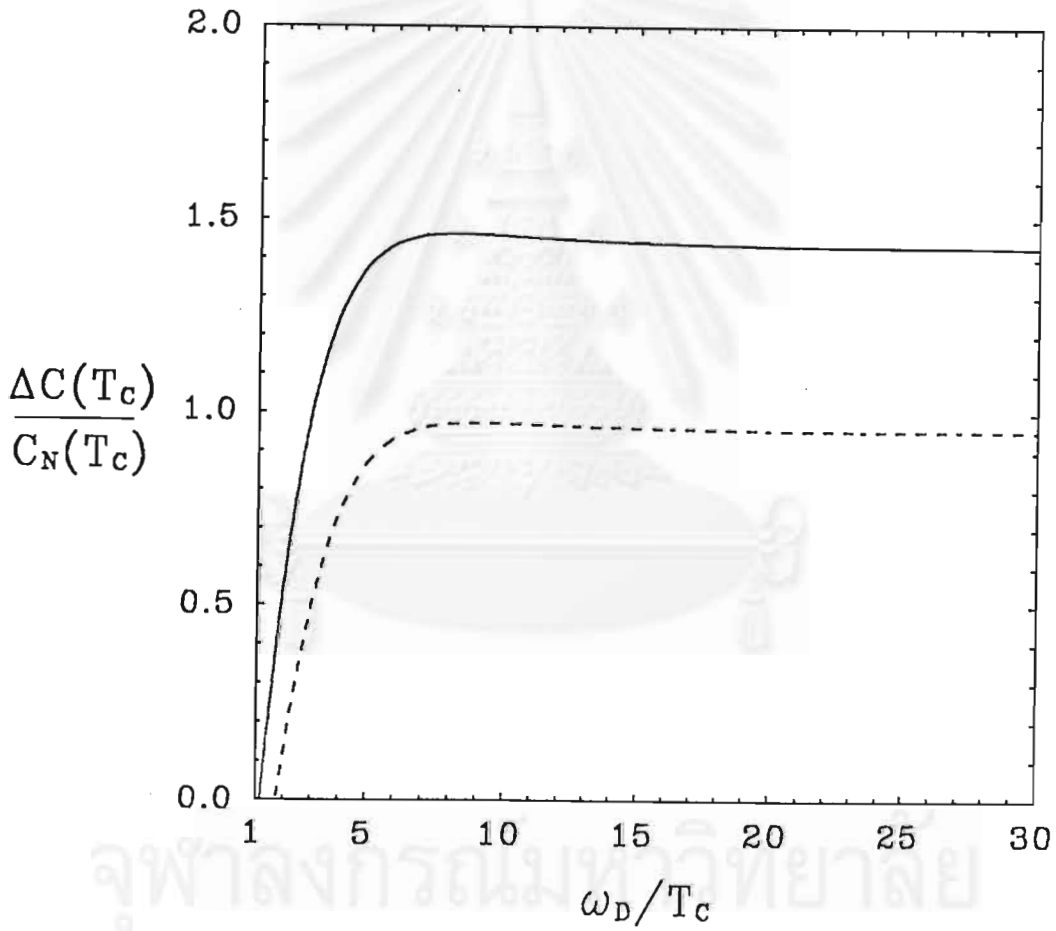

Figure 4.1: illustrates the jumps in specific heat, in units of the normal state specific heat at the transition temperature, versus ratio ω_D/T_c for the constant density of states at the Fermi level. The solid and dashed curves show results of calculations based upon s and d gaps, respectively.

As a matter of interest we also compute the jump in the specific heat for the d-wave superconductor. Taking $g(\phi) = \cos 2\phi$ for this case $\langle g^2(\phi)\rangle = 1/2$, $\langle g^4(\phi)\rangle = 3/8$, we find that the normalized jump in Eq.(4.24) gives the result

$$\frac{\Delta C(T_c)}{C_N(T_c)} = \frac{12}{\pi^2}\left\{\frac{\left(\frac{\omega_D}{2T_c}\right)^2\left[1+\tanh\left(\frac{\omega_D}{2T_c}\right)\right]-\left(\frac{\omega_D}{T_c}\right)\ln\left[2\cosh\left(\frac{\omega_D}{2T_c}\right)\right]+\mathrm{Li}_2\left[-e^{-\omega_D/T_c}\right]}{\frac{\tanh(\omega_D/2T_c)}{(\omega_D/2T_c)^2}-\frac{1}{(\omega_D/2T_c)}-\frac{2}{\pi^3}\sum_{n=0}^{\infty}\frac{1}{\left(n+\frac{1}{2}\right)^3}\tan^{-1}\left(\frac{(\omega_D/T_c)}{(2n+1)\pi}\right)}-\frac{\frac{2}{3}\tanh^2(\omega_D/2T_c)}{}\right\}. \tag{4.30}$$

This equation gives $\frac{\Delta C(T_c)}{C_N(T_c)} = 0.95$ in the limit $\omega_D/T_c \to \infty$. Graphical solution of $\frac{\Delta C(T_c)}{C_N(T_c)}$ vs. ω_D/T_c are plotted also in Fig. 4.1. Again we can see that the deviation of the ratio from the BCS result is significant for all ω_D/T_c values.

4.4 Effect of the Van Hove Singularity Density of States

However, if the density of states is energy-dependent such as in the case of Van Hove singularity, by taking $N(\varepsilon) = N(0)\ln\left|\frac{E_F}{\varepsilon}\right|$ in Eqs.(4.17) and (4.22), we get

$$C_N(T_c) = 8T_c N(0)\int_0^{\infty} dx \ln\left(\frac{E_F}{2T_c x}\right) x^2 \mathrm{sech}^2(x) \tag{4.31}$$

and

$$\frac{\Delta C(T_c)}{C_N(T_c)} = \frac{\int_0^{\omega_D/2T_c} dx \ln\left(\frac{E_F}{2T_c x}\right) x^2 \operatorname{sech}^2(x)}{\int_0^{\infty} dx \ln\left(\frac{E_F}{2T_c x}\right) x^2 \operatorname{sech}^2(x)} - 1 - \frac{\left[\left\langle g^2(\phi)\right\rangle \int_0^{\omega_D/2T_c} dx \ln\left(\frac{E_F}{2T_c x}\right) \operatorname{sech}^2(x)\right]^2}{\left\langle g^4(\phi)\right\rangle \int_0^{\infty} dx \ln\left(\frac{E_F}{2T_c x}\right) x^2 \operatorname{sech}^2(x) \int_0^{\omega_D/2T_c} dx \ln\left(\frac{E_F}{2T_c x}\right)\left[\frac{\operatorname{sech}^2(x)}{x^2} - \frac{\tanh(x)}{x^3}\right]}$$

(4.32)

By some procedures of integration, we obtain the formulas

$$\int_0^{\omega_D/2T_c} dx \ln\left(\frac{E_F}{2T_c x}\right) x^2 \operatorname{sech}^2(x) =$$

$$\ln\left(\frac{E_F}{2T_c}\right)\left\{\left(\frac{\omega_D}{2T_c}\right)^2\left[1+\tanh\left(\frac{\omega_D}{2T_c}\right)\right] - \left(\frac{\omega_D}{T_c}\right)\ln\left[2\cosh\left(\frac{\omega_D}{2T_c}\right)\right] + \frac{\pi^2}{12} + \mathrm{Li}_2\left[-e^{-\omega_D/T_c}\right]\right\}$$

$$-2\sum_{k=1}^{\infty}(-1)^{k-1}\left\{\begin{array}{l} e^{-k\omega_D/T_c}\left[-\frac{3}{4k^2} - \frac{\omega_D}{4kT_c} - \left(\frac{\omega_D}{2T_c}\right)^2 \ln\left(\frac{\omega_D}{2T_c}\right) - \frac{1}{k}\left(\frac{\omega_D}{2T_c}\right)\ln\left(\frac{\omega_D}{2T_c}\right)\right] + \frac{3}{4k^2} \\ + \sum_{n=0}^{\infty}\frac{(-1)^n(2k)^n}{k(n+1)!}\left(\frac{\omega_D}{2T_c}\right)^{n+1}\left[\ln\left(\frac{\omega_D}{2T_c}\right) - \frac{1}{n+1}\right] \end{array}\right\},$$

(4.33)

$$\int_0^{\infty} dx \ln\left(\frac{E_F}{2T_c x}\right) x^2 \operatorname{sech}^2(x) = \frac{\pi^2}{12}\ln\left(\frac{E_F}{2T_c}\right) - 0.2902, \tag{4.34}$$

$$\int_0^{\omega_D/2T_c} dx \ln\left(\frac{E_F}{2T_c x}\right) \operatorname{sech}^2(x) = \ln\left(\frac{E_F}{\omega_D}\right)\tanh\left(\frac{\omega_D}{2T_c}\right) + \frac{4}{\pi}\sum_{n=0}^{\infty}\frac{1}{(2n+1)}\tan^{-1}\left(\frac{\omega_D/\pi T_c}{2n+1}\right),$$

(4.35)

$$\int_0^{\omega_D/2T_c} dx \ln\left(\frac{E_F}{2T_c x}\right)\left[\frac{\operatorname{sech}^2(x)}{x^2} - \frac{\tanh(x)}{x^3}\right] =$$

$$\ln\left(\frac{E_F}{\omega_D}\right)\left[\frac{\tanh(\omega_D/2T_c)}{(\omega_D/2T_c)^2} - \frac{1}{(\omega_D/2T_c)}\right] - \frac{16}{\pi^3}\sum_{n=0}^{\infty}\frac{1}{(2n+1)^3}\tan^{-1}\left(\frac{\omega_D/T_c}{(2n+1)\pi}\right)\left[\ln\left(\frac{E_F}{\omega_D}\right)+1\right]$$

$$+\frac{16}{\pi^3}\sum_{n=0}^{\infty}\sum_{k=0}^{\infty}\sum_{m=1}^{k}\frac{1}{(2n+1)^3}\frac{(2k)!}{2^{2k}(k!)^2(2k+1)(2k-2m+1)}\tanh^{2k-2m+1}\left(\sinh^{-1}\left(\frac{\omega_D/T_c}{(2n+1)\pi}\right)\right)$$

$$-\frac{8}{\pi^2}\sum_{n=0}^{\infty}\frac{1}{(2n+1)^3}\sinh^{-1}\left(\frac{\omega_D/T_c}{(2n+1)\pi}\right) \tag{4.36}$$

and substituting these integral formulas in Eq.(4.32).

In the s-wave case, $g(\phi)=1$, the ratio between the specific heat jump and the normal phase specific heat of an s-wave Van Hove superconductor as

$$\frac{\Delta C(T_c)}{C_N(T_c)} = \frac{P(\omega_D,T_c,E_F)-Q(\omega_D,T_c,E_F)}{\frac{\pi^2}{12}\ln\left(\frac{E_F}{2T_c}\right)-0.2902} - 1 \tag{4.37}$$

where

$$P(\omega_D,T_c,E_F) =$$

$$\ln\left(\frac{E_F}{2T_c}\right)\left\{\left(\frac{\omega_D}{2T_c}\right)^2\left[1+\tanh\left(\frac{\omega_D}{2T_c}\right)\right]-\left(\frac{\omega_D}{T_c}\right)\ln\left[2\cosh\left(\frac{\omega_D}{2T_c}\right)\right]+\frac{\pi^2}{12}+\mathrm{Li}_2\left[-e^{-\omega_D/T_c}\right]\right\}$$

$$-2\sum_{k=1}^{\infty}(-1)^{k-1}\left\{\begin{array}{l} e^{-k\omega_D/T_c}\left[-\frac{3}{4k^2}-\frac{\omega_D}{4kT_c}-\left(\frac{\omega_D}{2T_c}\right)^2\ln\left(\frac{\omega_D}{2T_c}\right)-\frac{1}{k}\left(\frac{\omega_D}{2T_c}\right)\ln\left(\frac{\omega_D}{2T_c}\right)\right]+\frac{3}{4k^2} \\ +\sum_{n=0}^{\infty}\frac{(-1)^n(2k)^n}{k(n+1)!}\left(\frac{\omega_D}{2T_c}\right)^{n+1}\left[\ln\left(\frac{\omega_D}{2T_c}\right)-\frac{1}{n+1}\right] \end{array}\right\} \tag{4.38}$$

and

$$Q(\omega_D, T_c, E_F) =$$

$$\frac{\left(\ln\left(\frac{E_F}{\omega_D}\right)\tanh\left(\frac{\omega_D}{2T_c}\right) + 2\sum_{n=0}^{\infty}\frac{1}{\left(n+\frac{1}{2}\right)\pi}\tan^{-1}\left(\frac{\omega_D/T_c}{(2n+1)\pi}\right)\right)^2}{\left\{\begin{array}{l}\ln\left(\frac{E_F}{\omega_D}\right)\left[\frac{\tanh(\omega_D/2T_c)}{(\omega_D/2T_c)^2} - \frac{1}{(\omega_D/2T_c)}\right] - \frac{16}{\pi^3}\sum_{n=0}^{\infty}\frac{1}{(2n+1)^3}\tan^{-1}\left(\frac{\omega_D/T_c}{(2n+1)\pi}\right)\left[\ln\left(\frac{E_F}{\omega_D}\right)+1\right] \\ + \frac{16}{\pi^3}\sum_{n=0}^{\infty}\sum_{k=0}^{\infty}\sum_{m=1}^{k}\frac{1}{(2n+1)^3}\frac{(2k)!}{2^{2k}(k!)^2(2k+1)(2k-2m+1)}\tanh^{2k-2m+1}\left(\sinh^{-1}\left(\frac{\omega_D/T_c}{(2n+1)\pi}\right)\right) \\ - \frac{8}{\pi^2}\sum_{n=0}^{\infty}\frac{1}{(2n+1)^3}\sinh^{-1}\left(\frac{\omega_D/T_c}{(2n+1)\pi}\right)\end{array}\right\}}. \tag{4.39}$$

In the limit $\omega_D/T_c \to \infty$ when $E_F/T_c = 200$ and 50, Eqs.(4.37)-(4.39) gives $\frac{\Delta C(T_c)}{C_N(T_c)} = 1.94$ and 2.19, respectively (see Fig. 4.2).

For the d-wave, $g(\phi) = \cos 2\phi$, the normalized specific heat jump $\frac{\Delta C(T_c)}{C_N(T_c)}$ for a d-wave superconductor is calculated, and one obtains

$$\frac{\Delta C(T_c)}{C_N(T_c)} = \frac{6/\pi^2}{\ln\left(\frac{E_F}{T_c}\right) - 1.0458}\left\{P(\omega_D, T_c, E_F) - \frac{2}{3}Q(\omega_D, T_c, E_F)\right\} - 1 \tag{4.40}$$

with $P(\omega_D, T_c, E_F)$ and $Q(\omega_D, T_c, E_F)$ as defined in Eqs.(4.38) and (4.39), respectively. Results are presented in Fig. 4.2 for values of ω_D/T_c up to 25. In the limit $\omega_D/T_c \to \infty$ when E_F/T_c=200 and 50 Eq.(4.40) gives $\frac{\Delta C(T_c)}{C_N(T_c)} = 1.29$ and 1.46, respectively. In general, we can see that the normalized specific heat

jump for a d-wave superconductor is predicted to be much smaller than the BCS value of 1.43. However for an s-wave Van Hove superconductor the jump is significantly higher.

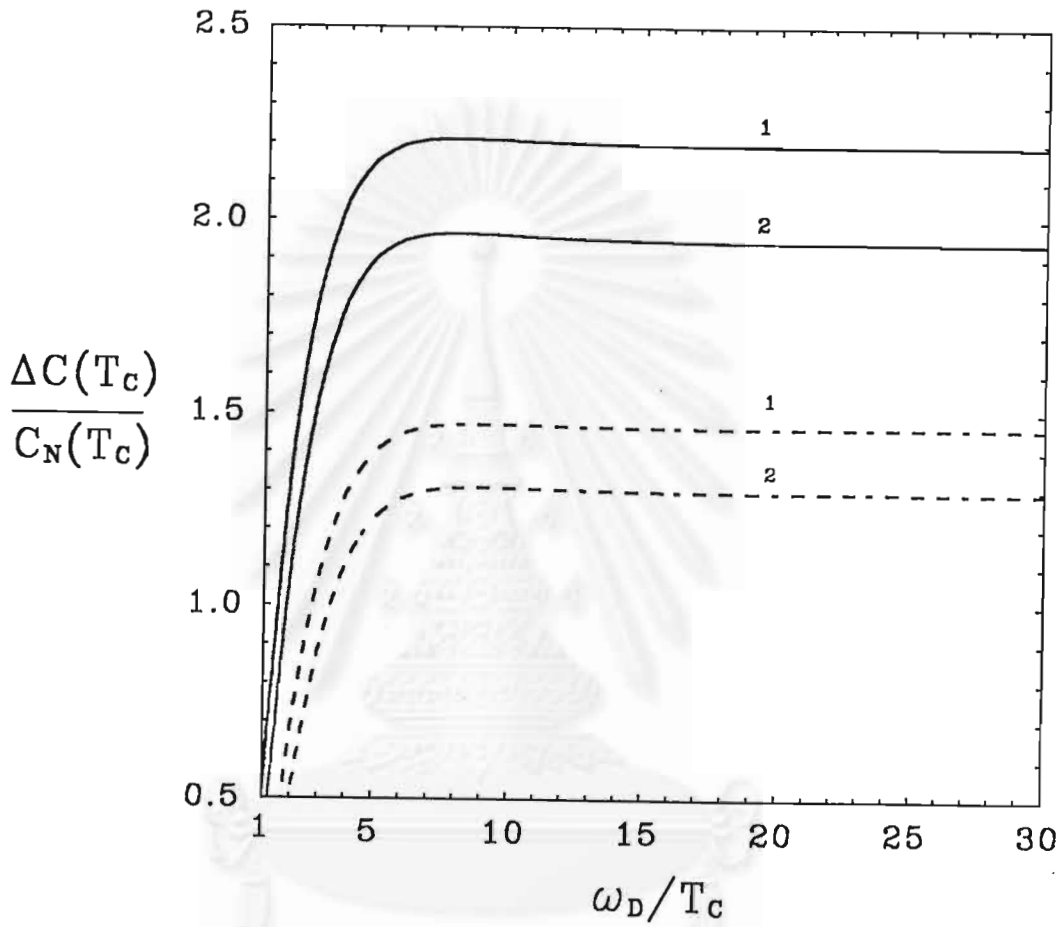

Figure 4.2: illustrates normalized electronic specific heat jump $\frac{\Delta C(T_c)}{C_N(T_c)}$ versus ratio ω_D/T_c of a Van Hove superconductor. The solid and dashed curves correspond to an s- and a d-wave gap symmetry, respectively. Curves 1 and 2 correspond to $E_F/T_c = 50$ and 200, respectively. Asymptotic values of $\frac{\Delta C(T_c)}{C_N(T_c)}$ for the s-wave in the limit $\omega_D/T_c \to \infty$ when $E_F/T_c = 50$ and 200 is 2.19 and 1.94, respectively and the d-wave case is 1.46 and 1.29, respectively.

Chapter 5

Discussion and Conclusions

In this thesis, we have studied the specific heat jump at critical temperature $\Delta C(T_c)$, in the constant density of states and the Van Hove singularity density of states based on the BCS framework. The effect of the pairing states both the isotropic s- wave and the anisotropic d- wave which have the influence on the symmetry of the energy gap is also investigated.

Our graphical solutions for the normalized specific heat jump help clarify how the jump is affected by the electronic density of states at the Fermi level, the symmetry of order parameters and material parameters. We can see that the deviations of the ratio $\frac{\Delta C(T_c)}{C_N(T_c)}$ from the canonical BCS value in high-T_c superconductors can be accounted for by considering either the symmetry of the gap or the VHS or the values of the parameters such as ω_D, T_c and E_F.

For the s-wave superconductors with the constant density of states, we derive an expression for the ratio between the jump in the specific heat at a transition from the normal to the superconducting states and the normal specific heat which is expressed by

$$\frac{\Delta C(T_c)}{C_N(T_c)} = \frac{12}{\pi^2}\left\{\begin{array}{l}\left(\frac{\omega_D}{2T_c}\right)^2\left[1+\tanh\left(\frac{\omega_D}{2T_c}\right)\right]-\left(\frac{\omega_D}{T_c}\right)\ln\left[2\cosh\left(\frac{\omega_D}{2T_c}\right)\right]+\mathrm{Li}_2(-e^{-\omega_D/T_c}) \\ -\dfrac{\tanh^2(\omega_D/2T_c)}{\dfrac{\tanh(\omega_D/2T_c)}{(\omega_D/2T_c)^2}-\dfrac{1}{(\omega_D/2T_c)}-\dfrac{16}{\pi^3}\sum_{n=0}^{\infty}\dfrac{1}{(2n+1)^3}\tan^{-1}\left(\dfrac{\omega_D/\pi T_c}{2n+1}\right)}\end{array}\right\}. \tag{5.1}$$

Our formula recovers the usual BCS result (1.43) by taking the limit $\omega_D/T_c \to \infty$ in Eq.(5.1). The fall of $\frac{\Delta C(T_c)}{C_N(T_c)}$ with decreasing ω_D/T_c is predicted when ω_D/T_c is less than or 7 as shown in Fig.4.1.

Recently Bandyopadhyay et al. (Bandyopadhyay et al., 1990) reported the results of specific heat results of specific heat measurements carried out on samples of Tl-based 2-2-2-3 compounds, their data for the average Debye temperature for 2-2-2-3 is 480 K. The T_c values of the 2-2-2-3 system are 107 and 125 K. They evaluated the BCS ratio $\frac{\Delta C(T_c)}{C_N(T_c)}$ for the system and found the ratios to be 1.45. This value is greater than our for the s-wave superconductor. Hence the Tl-system is not a simple BCS superconductor.

We have also studied $\frac{\Delta C(T_c)}{C_N(T_c)}$ as a function of ω_D/T_c for a d-wave superconductor having the constant density of states at the Fermi level. $\Delta C(T_c)$ and $C_N(T_c)$ are calculated using the exact expressions (4.21) and (4.11). The analytic expression for $\frac{\Delta C(T_c)}{C_N(T_c)}$ is

$$\frac{\Delta C(T_c)}{C_N(T_c)} = \frac{12}{\pi^2}\left\{ \frac{\left(\frac{\omega_D}{2T_c}\right)^2\left[1+\tanh\left(\frac{\omega_D}{2T_c}\right)\right]-\left(\frac{\omega_D}{T_c}\right)\ln\left[2\cosh\left(\frac{\omega_D}{2T_c}\right)\right]+\mathrm{Li}_2\left[-e^{-\omega_D/T_c}\right]}{-\dfrac{\frac{2}{3}\tanh^2(\omega_D/2T_c)}{\dfrac{\tanh(\omega_D/2T_c)}{(\omega_D/2T_c)^2}-\dfrac{1}{(\omega_D/2T_c)}-\dfrac{2}{\pi^3}\sum_{n=0}^{\infty}\dfrac{1}{\left(n+\frac{1}{2}\right)^3}\tan^{-1}\left(\dfrac{(\omega_D/T_c)}{(2n+1)\pi}\right)}} \right\}. \tag{5.2}$$

It is found that the d-wave symmetry lowers $\Delta C(T_c)$, hence the smaller value of the ratio $\frac{\Delta C(T_c)}{C_N(T_c)}$, this is probably due to the fact that there are a few more non-superconducting particles when a d-wave gap parameter opens compared to an s-wave gap. The limiting values of $\frac{\Delta C(T_c)}{C_N(T_c)}$ is 1.29 which is considerably lower than the BCS value of 1.43. The ratio of the specific heat jump $\frac{\Delta C(T_c)}{C_N(T_c)}$ versus ω_D/T_c for the d-wave gap parameter case is presented also in Fig.4.1. Our formula also predicts that the jump at T_c decreases when $\omega_D/T_c \leq 6$.

As for the VHS superconductor, we find that the effect of VHS on the electronic specific heat jump of an s-wave superconductor is to increase the value of the jump at T_c considerably over the BCS values according to Eq. (4.37).

$$\frac{\Delta C(T_c)}{C_N(T_c)} = \frac{P(\omega_D,T_c,E_F)-Q(\omega_D,T_c,E_F)}{\frac{\pi^2}{12}\ln\left(\frac{E_F}{2T_c}\right)-0.2902} - 1 . \tag{5.3}$$

The limiting value of $\frac{\Delta C(T_c)}{C_N(T_c)}$ with $\omega_D / T_c \to \infty$ is found to be 1.94 in fine agreement with Sarkar and Das who found the numerical value of the ratio at T_c to be 2.13 by using a more realistic density of states. Our result is also in agreement with Dorbolo et al. (Dorbolo et al., 1996, 1997) who in their study of the influence of a VHS on the ratio found the ratio at T_c to be 2, when they took $\Delta(0)$ to be 20 meV. We also found that the normalized ratio increases rapidly as ω_D / T_c increases from 1, reaches a maximum at ω_D / T_c=7 and as ω_D / T_c increases further, the normalized specific-heat jump remains unchanged. In addition our calculations show unambiguously that when the ratio E_F / T_c decreases, the jump ratio increases.

Finally the normalized specific heat difference for the d-wave VHS case has been calculated as Eq.(4.40)

$$\frac{\Delta C(T_c)}{C_N(T_c)} = \frac{6/\pi^2}{\ln\left(\frac{E_F}{T_c}\right) - 1.0458}\left\{P(\omega_D, T_c, E_F) - \frac{2}{3}Q(\omega_D, T_c, E_F)\right\} - 1 . \qquad (5.4)$$

It is presented in Fig.4.2. The graph shows that the normalized jump at T_c is much lower than the BCS values and that the magnitude of the jump is almost the same as that of the constant density of states case. Dorbolo et al. (Dorbolo et al., 1996, 1997) found that the ratio $\frac{C_S(T_c)}{C_N(T_c)}$ in a zero magnetic field in a d-wave superconductor with typical values of physical parameters in high-T_c superconductor is 1.4 which agrees well with our calculation here. We found

that as E_F/T_c decrease, the ratio $\frac{\Delta C(T_c)}{C_N(T_c)}$ increase. But for experimental data on $YBa_2Cu_3O_{7-\delta}$ (Junod et al., 1988), (Philips et al., 1990) obtained $\frac{\Delta C(T_c)}{C_N(T_c)} =$ 4.8, our theory cannot explain the result, this may be due to the fact that the high-T_c superconductor is not quite two-dimensional.

In conclusion, we would like to stress here that our calculation is strictly two-dimensional and our formula is valid when $\omega_D > T_c$. The case $\omega_D < T_c$ is unphysical, our graphs therefore start from $\omega_D/T_c \geq 1$. A test of the quantitative finding presented in this paper with respect to parameter changes can be made by varying the ratio ω_D/T_c and E_F/T_c. Should the test fails, we would need to conclude that the BCS theory that incorporates the VHS density of states is inapplicable to the material and that a new or modified density of states and theory are required.

จุฬาลงกรณ์มหาวิทยาลัย

References

Abramowitz, M., I. A. Stegun. Handbook of Mathematical Functions, New York: Dover, 1972. pp. 67, 1004.

Bandyopadhyay, A. K. et al. Physica C **165**, (1990): 29.

Bardeen, J., L. N. Cooper, and J. R. Schrieffer. Phys. Rev. **108**, (1957): 1175.

Bednorz, J. G., and K. A. Müller. Z. Phys. B **64**, (1986): 189.

Bednorz, J. G., and K. A. Müller. Rev. mod. Phys. **60**, (1988): 585.

Bogoliubov, N. N., D. N. Zubarev, and Yu. A. Tserkovnikov. Zh. Eksperim. i Teor. Fiz. **39**, 120 (1960); Soviet Phys. JETP **12**, (1961): 88.

Chu, C. W., L. Gao, F. Chen, Z. J. Huang, R. L. Meng, and Y. Y. Xue. Nature. **365**, (1993): 323.

Dagotto, E., A. Nazarenko, and M. Boninsegni. Phys. Rev. Lett. 74, (1995): 2841.

Dessau, D. S., Z. X. Shen, D. M. King, D. S. Marshall, L. W. Lombardo, P. H. Dickinson, A. G. Loeser, J. DiCarlo, C. H. Park, A. Kapitulink, and W. E. Spicer. Phys. Rev. Lett. **71**, (1993): 2781.

Dorbolo, S., M. Houssa, and M. Ausloos. Physica C **267**, (1996): 24.

Dorbolo, S. Physica C **276**, (1997): 175.

Fröhlich, H. Phys. Rev. **79**, (1950): 845.

Friedel, J. J. Phys. Condens. Matter **1**, (1989): 7757.

Gama Goigochea, A. Phys. Rev. B **49**, (1994): 6864.

Gradshteyn I. S., and I. M. Ryzhik. Table of Integrals Series and Products, New York: Academic, 1965. pp. 214, 242.

Geilikman, B. T., and V. Z. Kresin. Fiz. Tverd. Tela **5**, 3549 (1963); Soviet Phys. Solid State **5**, (1964): 2605.

Geilikman, B. T., and V. Z. Kresin. Zh. Eksperim. i Teor. Fiz Pis'ma **3**, 48 (1966); Soviet Phys. JETP Letters **3**, (1966): 28.

Gofron, K., J. C. Campuzano, A. A. Abrikosov, M. Lindroos, A. Bansil, H. Ding, D.Koelling, and B. Dobrowski. Phys. Rev Lett. **73**, (1994): 3302.

Gopal, E. S. R. Specific heat at low temperature, London: Heywood, 1996.

Hermann, A. M., and J. V. Yakhmi. (eds) Thallium-Based High Temperature Superconductors, New York: Marcel Dekker, 1994.

Hirsch J. E., and D. J. Scalapino. Phys. Rev. Lett. **56**, (1986): 2732.

Houssa, M., M. Ausloos, and R. Cloots. Phys. Rev. B **56**, (1997): 6226.

Junod, A. et al. Physica C **152**, (1988): 495.

Junod, A. Physical properties of high temperature superconductors II, Ed. D. M. Ginsberg, Singapore: Scientific, 1990. pp. 13.

King D. M., Z. X. Shen, D. S. Dessau, B.O. Wells, W. E. Spicer, A. J. Arko, D. S. Marshall, J. Dicarlo, A. G. Loeser, C. H. Park, E. R. Ratner, J. L. Peng, Z.Y. Li, R. L. Greene. Phys. Rev. Lett. **70**, (1993): 3159.

Krunavakarn, B., P. Udomsamuthirun, S. Yoksan, I. Grosu, and M. Crisan. J. Supercond. **11**, (1998): 271.

Labbe′, J., and J. Bok. Europhys. Lett. **3**, (1987): 1225.

Madelung, O. Introduction to Solid-State Theory, Springer-Verlag Berlin New York: Heidelberg, 1978.

Ma, J., C. Quitmann, R. J. Kelley, P. Almeras, H. Berger, G. Margaritondo, and M. Onellion. Phys. Rev. B **51**, (1995): 3832.

Maple, M. B. J. of Magnetism and Magnetic Materials **117-181**, (1998): 18.

Markiewicz, R. S. J. Phys. Condens. Matter **2**, (1990): 665.

Markiewicz, R. S. Physica C **200**, (1992): 65.

Maxwell, E. Phys. Rev. **78**, (1950): 477.

Melik-Barkhudarov, T. K. Fiz. Tverd. Tela **7**, (1965): 1368; Soviet Phys.-Solid State **7**, (1965): 1103.

Mühlschlegel, B. Z. Physik **155**, (1959): 313.

Newns, D. M., C. C. Tsuei, P. C. Pattnaik, and C. L. Kane. Comments Condens. Matter Phys. **15**, (1992): 273.

Newns, D. M., C. C. Tsuei, R. P. Huebener, P. J. M. van Bentum, P. C. Pattnaik, and C. C. Chi. Phys. Rev. Lett. **73**, (1994): 1695.

Pakokthom, C., B. Krunavakarn, P. Udomsamuthirun, and S. Yoksan. J. Supercond. **11**, (1998): 429.

Parks, R. D. Superconductivity, Marcel New York: Dekker, 1969.

Phillips, N. E., R. A. Fisher, J. E. Gordon, S. Kim, and A. M. Stacy. Phys. Rev. Lett. **65**, (1990): 357.

Pokrovskii, V. L., and M. S. Ryvkin. Zh. Eksperim. i Teor. Fiz. **43**, 89 (1962); Soviet Phys. JETP **16**, (1963): 65.

Reynolds, C. A., B. Serin, W. H. Wright, and L. B. Nesbitt. Phys. Rev. **78**, (1950): 487.

Schilling, A., M. Cantori, J. D. Guo, and H. R. Ott. Nature **363**, (1993): 56.

Sarkar, S., and A. N. Das. Phys. Rev. B **54**, (1996): 14974.

Sonier, J. E., R. F. Kiefl, J. H. Brewer, D. A. Bonn, J. F. Carolan, K. H. Chow, P. Dosanjh, W. N. Hardy, Ruixing Liang, W. A. MacFarlane, P. Mendels, G.D. Morris, T. M. Riseman, and J. W. Schneider. Phys. Rev. Lett. 72, (1994): 744.

Takigawa, M, and D. B. Mitzi. Phys. Rev. Lett. **73**, (1994): 1287.

Takigawa, M., J. L. Smith, and W. L. Hults. Phys. Rev. B **44**, (1991): 7764.

Tsuei, C. C., C. C. Chi, D. M. Newns, P. C. Pattnaik, and M. Dä umling. Phys. Rev. Lett. **69**, (1992): 2134.

Tsuei, C. C., D. M. Newns, C. C. Chi, and P. C. Pattnaik. Phys. Rev. Lett. **65**, (1990): 2724.

Tsuei, C. C., J. R. Kirtley, C. C. Chi, Lock See Yu-Jahnes, A. Gupta, T. Shaw, J. Z. Sun, and M. B. Ketchen. Phys. Rev. Lett. **73**, (1994): 593.

Van Hove, L. Phys. Rev. **89**, (1953): 1189.

Wada, Y. Phys. Rev. **135**, (1964): A1481.

Waldram, J. R. Superconductivity of Metals and Cuprates, Bristol: Adam Hilger, 1996.

Wang, Z. D., N. Z. Zou, J. Z. Pang, and C. D. Gong, Solid State Commun. **64**, (1987): 531.

Wollman, D. A., D. J. Vanharlingen, W. C. Lee, D. M. Ginsberg, A. J. Leggettt. Physica B **194-196**, (1994): 1669.

Wu, M. K., J. R. Ashburn, C. J. Torng, P. H. Hor, R. L. Meng, L. Gao, Z. J. Huang, Y. Q. Wang, and C. W. Chu. Phys. Rev. Lett. **58**, (1991): 908.

สถาบันวิทยบริการ
จุฬาลงกรณ์มหาวิทยาลัย

Curriculum Vitae

Mr. Suchat Kaskamalas was born on August 18, 1975 in Bangkok. He received his B.Sc. degree in physics from Srinakharinwirot University in 1997.

Publication List

1. Kaskamalas, S., B. Krunavakarn, P. Rungruang, and S. Yoksan. Dependence of the Gap-Ratio on the Fermi Level Shift in a Van Hove Supeconductor. Journal of Superconductivity: Incorporating Novel magnetism **13**, 33 (2000).
2. Krunavakarn, B., S. Kaskamalas, N. Jinuntuya, and S. Yoksan. Specific Heat Jump at T_c of High-T_c Superconductors: Effect of Van Hove Singularity. Journal of Superconductivity: Incorporating Novel magnetism **13**, 41 (2000).

หอสมุดกลาง สถาบันวิทยบริการ จุฬาลงกรณ์มหาวิทยาลัย

จุฬาลงกรณ์มหาวิทยาลัย